MASTERARBEIT | MASTER'S THESIS

Titel | Title

Assessing the inhibitory potential of three biological nitrification inhibitors on an agricultural soil from Linz, Austria

verfasst von | submitted by

Konstanze Kamilla Madani BSc

angestrebter akademischer Grad | in partial fulfilment of the requirements for the degree of

Master of Science (MSc)

Wien | Vienna, 2024

Studienkennzahl lt. Studienblatt | Degree programme code as it appears on the student record sheet:	UA 066 830
Studienrichtung lt. Studienblatt | Degree programme as it appears on the student record sheet:	Masterstudium Molecular Microbiology, Microbial Ecology and Immunobiology
Betreut von | Supervisor:	Univ.-Prof. Dipl.-Biol. Dr. Holger Daims

universität wien

Contents

1 Abstract - german

Der Prozess der Nitrifikation ist ein entscheidender Schritt im Stickstoffkreislauf, der die Oxidation von Ammoniak (NH_3) zu Nitrat (NO_3^-) durch Mikroorganismen wie ammoniakoxidierende Bakterien (AOB), ammoniakoxidierende Archaeen (AOA) und vollständige Ammoniakoxidierer (Comammox) umfasst. Obwohl dieser Prozess für den Nährstoffkreislauf unerlässlich ist, stellt er eine Herausforderung für die Umwelt dar, insbesondere in landwirtschaftlichen Systemen, in denen reaktiver Stickstoff aufgrund von Düngung in großen Mengen vorhanden ist. In diesen Systemen können Prozesse wie Nitratauswaschung zu einer Verunreinigung des Grundwassers und zu erhöhten Treibhausgasemissionen, insbesondere Lachgas (N_2O), führen. Um diesen Problem entgegenzuwirken, werden synthetische Nitrifikationshemmer eingesetzt, die die Umwandlung von Ammoniak in Nitrat verlangsamen und so die Umweltauswirkungen von Stickstoffdüngern verringern.
Als nachhaltige Alternative, zeichnen sich biologische Nitrifikationsinhibitoren (BNIs) ab, da es sich um natürliche, von Pflanzen produzierte Verbindungen handelt, die ebenso Nitrifikation unterdrücken können. Die Wirksamkeit von BNIs kann jedoch je nach Bodenbeschaffenheit, Zusammensetzung der mikrobiellen Gemeinschaft und Umweltbedingungen erheblich variieren. Ein klares Verständnis des Einflusses dieser Faktoren ist für eine wirksame Anwendung von BNIs in der Landwirtschaft unerlässlich.
In dieser Studie bewerteten wir die Wirksamkeit von drei BNIs (MHPP, MHPA und Limonen) durch die Bestimmung ihrer effektiven Konzentration 50 (EC50) in landwirtschaftlichen Böden aus Linz, Österreich. Die Ergebnisse dieser Studie werden mit anderen Studien in Relation gesetzt, die von Rojas et al. (2023) an landwirtschaftlichen Böden aus dem Marchfeld und Wieselburg, Österreich, durchgeführt wurden. Die Ermittlung der Effizienz wurde durch die Inkubation von Boden-Wasser gemischen mit verschiedenen Konzentrationen der jeweiligen BNIs und der anschließende fluorometrische Analyse der Nitratakkumulation bewertet. Wir zeigen, dass die BNI-Effizienz in verschiedenen Böden stark variiert, und zeigen Korrelationen zu Bodeneigenschaften wie pH-Wert, Kupfer-, Ton- und Natriumgehalt sowie C-gehalt.
Darüber hinaus haben wir 16S rRNA- und *amoA*-Gen-amplikon-sequenzierung verwendet, um die Zusammensetzung der mikrobiellen Gemeinschaft und die Verteilung der wichtigsten Taxa zu bewerten. q QPCR wurde zur Quantifizierung der gesamten mikrobiellen Gemeinschaft und verschiedener ammoniakoxidierender Gilden durchgeführt. Unsere Ergebnisse zeigen eine große Vielfalt innerhalb von AOA, während AOB und Comammox - gruppe B überwiegend von einzelnen Taxa dominiert wurden.
Diese Studie unterstreicht, die Wichtigkeit der Berücksichtigung bodenspezifischer Faktoren, um eine breitentaugliche Anwendung zu gewährleisten und letztlich zu nachhaltigeren landwirtschaftlichen Praktiken beizutragen.

2 Abstract

Nitrification is a critical step in the nitrogen cycle, involving the oxidation of ammonia (NH_3) to nitrate (NO_3^-) by microorganisms such as ammonia-oxidizing bacteria (AOB), ammonia-oxidizing archaea (AOA), and complete ammonia oxidizers (comammox). Although this process is essential for nutrient cycling, it presents environmental challenges, especially in agricultural systems where reactive nitrogen is present in high quantities due to fertilization. In these systems, nitrate leaching can lead to groundwater contamination and increased greenhouse gas emissions, particularly nitrous oxide (N_2O). To mitigate these issues, nitrification inhibitors (NIs) are employed to slow the conversion of ammonia to nitrate, thereby reducing the environmental impact of nitrogen fertilizers. Biological nitrification inhibitors (BNIs) have emerged as a promising alternative to synthetic nitrification inhibitors (SNIs), as they are natural compounds produced by plants that can suppress nitrification. However, the effectiveness of BNIs can vary significantly depending on soil characteristics, microbial community composition, and environmental conditions. Understanding these factors is essential for the effective application of BNIs in agriculture. In this study, we evaluated the efficiency of three BNIs (MHPP, MHPA, and limonene) by determining their effective concentration 50 (EC50) in agricultural soil from Linz, Austria. We compared these results with similar studies conducted on agricultural soils from Marchfeld and Wieselburg, Austria by Rojas et al. (2023). Efficiency was assessed through soil slurry incubation followed by fluorometric analysis of nitrate accumulation. We show that BNI efficiency is highly variable across soils and propose correlations to soil characteristics like pH, copper, clay, and sodium content as well as total carbon. Additionally, we utilized 16S rRNA and *amoA* gene amplicon sequencing to assess microbial community composition and the distribution of key taxa. We also performed qPCR for the quantification of the total microbial community and different ammonia oxidizing guilds. Our results reveal a broad diversity within AOA, while AOB and comammox bacterial clade B were predominantly dominated by single taxa. This study underscores the importance of accounting for soil-specific factors to pave the way for the widespread application of BNIs, ultimately contributing to more sustainable agricultural practices.

3 Introduction

3.1 Nitrogen cycle

Nearly three-quarters of the earth's atmosphere is composed of nitrogen gas (N_2) [1], making nitrogen one of the most abundant elements on our planet. Despite its wide distribution, most of the present nitrogen is not accessible to organisms, as the majority of it exists in its molecular form (N_2), wherein two nitrogen atoms are held together by a strong triple bond (945.4 kJ/mol). Breaking this bond demands a considerable amount of energy, which can only be accessed through specific nitrogen-fixing organisms or high-temperature processes. The collective amount of nitrogen (N) in the earth's atmosphere, soils, and waters is approximately 4×10^{21} grams, surpassing the combined mass of carbon, oxygen, sulfur, and phosphorus [2]. Given its widespread distribution, microorganisms have developed pathways to utilize the diverse range of nitrogen compounds and their redox potential as an energy source [3]. These microbially mediated pathways facilitate nitrogen recycling in ecosystems and constitute the biogeochemical nitrogen cycle. This cycle comprises three main closely interconnected parts: N_2 fixation, nitrification, and denitrification. Apart from N_2 fixation, these processes are exclusively carried out by microorganisms consisting of nitrogen fixers, nitrifiers, and denitrifiers.

3.1.1 Nitrogen fixation

Nitrogen fixation entails converting elemental N_2 by incorporating nitrogen into ammonia (Figure 1.1). This energy-intensive process is typically carried out by highly specialized organisms or through substantial energy inputs, such as lighting. Additionally, high amounts of N are present in the earth's inner layer and can be transported to the surface and atmosphere through volcanic eruptions. Prominent organisms capable of nitrogen fixation include *Cyanobacteria* in aquatic systems. They fix nitrogen using an oxygen-sensitive enzyme, called nitrogenase. To mitigate its vulnerability to oxygen, they have evolved mechanisms to protect the enzyme, such as temporal decoupling or spatial separation [1]. In soil, symbiotic microorganisms, often attached to root systems, like *Rhizobia*, *Frankia*, *Azotobacter*, *Clostridium*, and *Klebsiella* can fix nitrogen.

3.1.2 Nitrification

Nitrification is the process of oxidizing ammonia (NH_3), to nitrate (NO_3^-) (Figure1.2). This process is carried out by chemolithoautotrophic and chemoorganotrophic (heterotrophic) microorganisms which vary greatly in their preferred carbon source and electron reductants. Ammonia oxidizing bacteria (AOB), ammonia-oxidizing archaea (AOA), comammox as well as nitrite-oxidizing bacteria (NOB) belong to the chemolithoautotrophic organisms, meaning that they use CO_2 or HCO_3^- as their main carbon source [4, 5]. AOA and AOB undertake the initial step of nitrification, converting ammonia (NH_3) which is the lowest oxidized form of nitrogen into nitrite (NO_2^-) via hydroxylamine and enzyme-bound HNO and NO intermediates [6]. En-

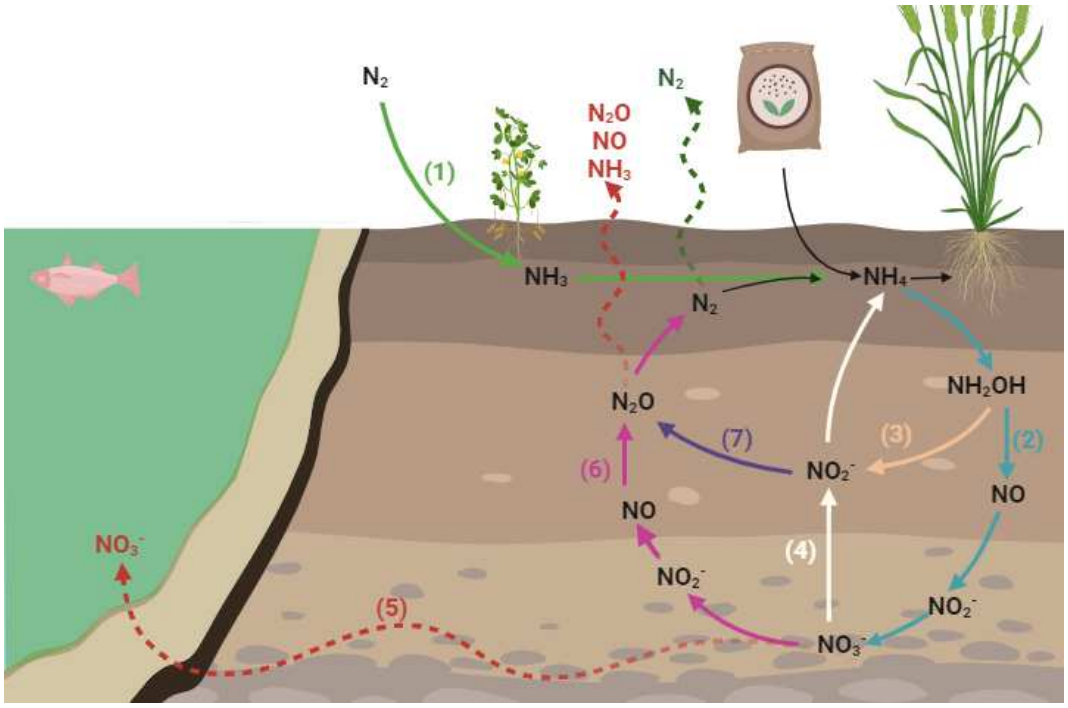

Figure 1: Microorganisms transform nitrogen through redox reactions. Atmospheric nitrogen (N_2) is reduced to ammonia (NH_3) by diazotrophs and then protonated to ammonium (NH_4^+) **(1)**. Ammonium is oxidized to nitrate (NO_3^-) **(2)**. In unfavorable conditions for nitrifying bacteria, partial nitrification can also be performed by other microbial taxa **(3)**. NO_3^- can leach from the soil, leading to eutrophication **(5)**, be reduced to ammonium via dissimilatory nitrate reduction (DNRA) **(4)**, or be reduced to nitrous oxide (N_2O) by denitrifying taxa and subsequently to N_2 to complete the full nitrogen cycle **(6)**. During **(6)** gaseous compounds like N_2O, NH_3, and NO can be released. Additionally, nitrifier denitrification can occur **(7)**.

zymes AMO (ammonia monooxygenase) and HAO (hydroxylamine oxidoreductase) drive these steps. After this, nitrite-oxidizing bacteria (NOB) convert NO_2^- to nitrate NO_3^-, mediated by the nitrite oxidoreductase (NXR) enzyme.

This process was formerly believed to be an obligate two-step process, involving AOA/AOB followed by NOBs for complete NH_4^+ to NO_3^- transformation. However, a new functional clade, comammox (complete ammonia oxidizing bacteria) from the *Nitrospira* genus, capable of independently conducting both steps, was discovered in 2015 [7, 8].

In anoxic environments, anaerobic litho-autotrophic bacteria can also oxidize ammonia (Anammox). They can use NO_2^- as an electron acceptor and produce N_2 [9]. Although anammox bacteria are thought to be obligately anaerobic they have a tolerance of oxygen and are therefore prevalent in different soils [10].

Beyond autotrophic microorganisms conducting aerobic and anaerobic nitrification, heterotrophic nitrification constitutes a third process for NO_3^- production in soils. Various fungi and heterotrophic bacteria can generate NO_2^- or NO_3^- utilizing NH_4^+ or organic N as substrates [11]. Although these organisms use an AMO-like enzyme, they differ greatly from canonical nitrifiers

as their main substrate is NH_4^+ [12].

3.1.3 Denitrification and dissimilatory nitrate reduction to ammonium (DNRA)

Denitrification is the stepwise conversion of NO_3^- to NO_2^-, nitric oxide (NO), and nitrous oxide (N_2O) into dinitrogen (N_2) and is executed by a wide range of bacteria (Figure1.6). This process is thought to be an anaerobic process as some of the enzymes involved in this pathway are oxygen-sensitive [13]. Nevertheless, some gram-negative bacteria, belonging to the phylum Proteobacteria, can also conduct this process under aerobic conditions [14]. Organisms capable of carrying out the entire process of converting NO_3^- to N_2 are termed canonical denitrifiers. Many heterotrophic microbes only possess incomplete denitrification pathways and don't produce N_2 as an end product but gaseous nitrogen-compounds like NO and N_2O, which are environmental pollutants [15] (Figure1.5).
Another possible fate of NO_3^- is the DNRA pathway, a process resulting from anaerobic respiration by chemoorganoheterotrophic microbes that use NO_3^- as an electron acceptor (Figure.1.4). Under anaerobic conditions, these microbes oxidize organic matter and utilize NO_3^-, instead of oxygen, as the electron acceptor, reducing it first to NO_2^- and then to ammonium ($NO_3^- \rightarrow NO_2^- \rightarrow NH_4^+$).

3.2 Nitrification in soil

The process of nitrification is essential across all ecosystems. Emphasizing its critical importance and widespread occurrence, recent studies indicate a significant functional redundancy within nitrifying communities [16]. This observation is further bolstered by research demonstrating that reductions in soil microbial diversity do not substantially impact the nitrification process [17], pointing out the high resilience and significance of this process. Ammonia oxidizers typically attach to negatively charged soil particles, which enhances their resistance to water flow and contributes to community stability [18]. This stable microenvironment supports a greater species diversity [18]. Moreover, the attachment of positively charged NH_4^+ ions to soil particles provides ammonia-oxidizing bacteria with proximity to their energy source, further optimizing their ecological niche. In this sense, it comes as no surprise, that more than one microbial clade developed mechanisms to perform the nitrification process. Representatives of ammonia-oxidizing archaea (AOA) and bacteria (AOB, comammox) are found all over the globe and inhabit every ecosystem, while environmental parameters select for either clade.
Among these influencing factors, pH often plays a significant role. It does not only impact the growth of nitrifying organisms but also affects the availability of reactive nitrogen compounds as the NH_4^+/NH_3 equilibrium is highly dependent on the pH [19]. In most natural systems, reactive N exists primarily in its positively charged ion form, ammonium (NH_4^+). However, the enzyme responsible for the initial step of the reaction utilizes NH_3, the gaseous form of ammonia, which typically remains a minor component at equilibrium. At low pH, the equilibrium shifts towards NH_4^+, lowering the NH_3 concentration, which favors AOA as their AMO has a high affinity towards NH_3 and can therefore still work efficiently under low NH_3 concentrations. In general, AOA is hence thought to dominate acidic soils [20] while AOB dominates neutral

soils [14]. In this sense, AOBs typically tend to prevail in systems that receive substantial direct inputs of inorganic ammonia, like agricultural systems that undergo fertilization, while AOA dominates in low $NH_4{}^+$+ environments [21]. Additionally, while the AOA AMO, demonstrates a stronger affinity for $NH_4{}^+$, it exhibits a lower maximum rate of ammonia oxidation. As a result, their AMO becomes saturated more readily, rendering them less efficient in utilizing high concentrations of ammonia [22].
While establishing an ideal pH for maximizing nitrification has posed challenges, research has revealed intriguing insights. Laboratory studies with pure cultures have highlighted nitrifying organisms' low tolerance to acidic conditions. However, field studies in whole soil systems present a contrasting picture, showing significant nitrification activity even at low pH levels. This apparent discrepancy may be attributed to microenvironments within the soil, maintaining higher pH values and thereby supporting nitrification [23]. Despite this complexity, a general pH range conducive to nitrification, typically falling between approximately 5 to 8, has been identified, providing optimal conditions for the nitrification process [23].
Additionally, the quantity and composition of soil water are vital determinants of the nitrification rate as in soils with high water content, oxygen availability may become limited. The soils water content is strongly influenced by the physical composition of the soil. Soils with a high clay content can retain more water, influencing the soil's moisture content and, in turn, affecting its aeration. As nitrification is an aerobic process this lack of oxygen can limit its productivity [24]. Besides affecting the soil water content, studies suggest, that soils with a high clay content additionally mitigate nitrification by retaining organic N by the clay particles therefore making it less vulnerable to microbial usage[25]. Furthermore, high temperatures can aggravate this issue by reducing the solubility of oxygen and increasing the consumption rate by other heterotrophic microbes [23]. In general, the physical soil composition heavily affects the nitrification process, and soil characterization components have to be taken into account when studying the nitrification potential of a specific soil.

3.2.1 AOB

AOBs are gram-negative bacteria, belonging to the genera *Nitrosomonas* and *Nitrosospira*. They can be described as chemolithoautotrophs, meaning that they obtain energy from the oxidation of inorganic compounds (such as NH_3) and use CO_2 as their carbon source. Although AOBs are obligate aerobes, they can survive under anaerobic conditions by using hydroxylamine or ammonia as an electron doner. Under anaerobic conditions, this process is thought not to provide sufficient energy for cell growth but it generates enough energy for the maintenance of cell functions[26]. In soil, Betaproteobacteria are responsible for the vast majority of ammonia oxidation, usually dominated by *Nitrospira*[18].

3.2.2 AOA

The discovery of the archaeal AMO and its widespread distribution has revolutionized our understanding of the nitrogen cycle and its participants. They are found in the phylum Thermoproteta, class *Nitrosphaeria*, and order *Nitrosphaerales*. In many habitats, such as soil, the abundance of AOA far surpasses that of AOB, underscoring the possible significance of archaeal nitrification

[27, 28]. A distinctive feature of archaea is their capacity to thrive under extreme conditions. In this regard, AOA inhabit a broad range of habitats, surpassing the scope of their bacterial counterparts, and even represent the most abundant archaeal clade in soils [29, 30, 31, 5, 32]. AOA dominance is particularly notable in acidic soils [33], which would explain high nitrification rates in acidic environments. The biochemistry of AOAs differs from that of AOBs, as AOA lack the HAO and any homologous enzymes are absent from their genome [34].

3.2.3 Comammox

Because of the advantageous bioenergetics associated with complete NH_3 oxidation, the existence of comammox bacteria has been hypothesized for a considerable period [35]. In 2015, two research groups discovered them inside the bacterial genus *Nitrospira* [7, 8]. These organisms contain AMO, HAO, and additionally NXR genes and are therefore capable of complete NH_3 oxidation. Since their discovery, they have been found in multiple environments including soil, where *Nitrospira* are found in large abundances [36]. The phylogenetic analysis places them in two distinctive clades (clade A, clade B) while only clade B is found to be active in soils [37, 38]. While falling under the bacterial clade, their approach aligns more with the AOA strategy, exhibiting a preference for lower NH_3 concentrations and achieving a higher yield in comparison to their counterparts [22].

3.2.4 NOB

Nitrite-oxidizing bacteria form a diverse group, encompassing representatives from seven bacterial genera: *Nitrobacter*, *Nitrospira*, *Nitrotoga*, *Nitrococcus*, *Nitrospina*, *Nitrolancetus*, and *Nitromaritima* [39]. Despite their shared process of oxidizing NO_2^- to NO_3^- through the NXR, these bacteria employ different strategies. *Nitrobacter* for instance is considered an r-strategist, thriving in environments with high NO_2^- concentrations, while *Nitrospira* belongs to K-strategists and is well adapted to low NO_2^- concentrations [40, 41]. These variations in NXR affinities for NO_2^- are likely attributed to differences in cellular localization [42].

3.3 Agricultural Revolution - The Haber-Bosch process

Addressing the scarcity of reactive nitrogen (Nr) in soil [43], the discovery of the Haber-Bosch process in 1908 brought about a revolution in agricultural productivity [1]. This chemical process converts N_2 and hydrogen gas (H_2) into ammonia under high pressure and temperature [44].

$$N_2 + 3H_2 = 2NH_3$$

Consequently, crop growth was no longer limited by nitrogen availability. This innovation is estimated to account for half of the Earth's population being supported by the surplus crops resulting from increased nitrogen availability [44]. In fact, in 2010, the nitrogen fixation achieved through the Haber-Bosch process (120 Tg N per year) was twice the amount fixed by natural

terrestrial sources (63 Tg N per year) [45].

However, the process of nitrification reduces the effectiveness of added NH_4^+ in fertilizers, as nitrifying organisms swiftly convert ammonium into NO_3^-. In this form, the nitrogen often either becomes inaccessible or less favorable to plants or is easily lost via leaching, resulting in its "loss" for agricultural purposes. This loss affects up to approximately 50-70% of the nitrogen added through fertilizers [46, 47, 18]. To combat this issue, besides adapting application techniques [48] and developing new fertilizer technologies [49, 50], a common approach has been to increase the application of nitrogen to ensure that plants receive an adequate supply. However, the products of nitrification are often compounds that can be detrimental to the ecosystem, especially in high dosages. Subsequently, with the increased amount of fertilizer nitrogen, the amount of incriminatory compounds has increased concurrently. It is projected that around 61.5 Tg N per year will be lost through NO_3^- conversion by 2050 [51].

Due to its negative charge, NO_3^- is prone to leaching. It can easily dissolve in water and can be transported by rainwater or runoff into water bodies such as streams, rivers, lakes, and groundwater [52] (Figure1.5). Elevated NO_3^- concentrations in aquatic systems can result in eutrophication, a process where excessive nutrients stimulate the growth of algae and aquatic plants [53]. As these organisms flourish and deplete oxygen levels, "dead zones" devoid of aquatic life emerge and substantially decrease ecosystem biodiversity. Additionally, NO_3^- can accumulate in groundwater and can therefore enter the human food chain, causing health hazards for infants (blue baby syndrome) and stomach cancer [54].
Another reactive N-compound, that drastically increased with anthropogenic Nr production is N_2O. Due to its ability to absorb infrared light, which reduces the escape of thermal radiation from the Earth's surface into the atmosphere, it acts as a potent greenhouse gas (Figure 1.5) [55, 56, 46]. Additionally, N_2O plays a critical role in the catalytic destruction of the ozone layer [54]. With a global warming potential 310 times greater than carbon dioxide (CO_2) [57, 58], and a long atmospheric lifetime of 150 years [59], N_2O significantly contributes to the greenhouse effect. According to Crutzen and Ehhalt (1977), a doubling of atmospheric N_2O concentrations could deplete the stratospheric ozone layer by 10%, leading to a 20% increase in ultraviolet radiation reaching the earth's surface.
The primary sources of N_2O in soils are biological nitrogen transformation processes, specifically nitrification and denitrification[60]. In aerobic soil compartments, N_2O is produced as a non-obligate intermediate during autotrophic nitrification, particularly during the oxidation of hydroxylamine by the enzyme hydroxylamine oxidoreductase (HAO) [60]. In contrast, in anaerobic soil compartments, denitrification is the dominant process responsible for N_2O production [61].
In AOB N_2O gas can be produced via the chemical decomposition of NH_2OH to NO and N_2O [57]. In AOA the production of N_2O gas is not as well-defined. Nevertheless, AOA and AOB show differences in the amount of N_2O produced as AOB are thought to produce around 50 % more N_2O gas than AOA [62]. Considering that AOBs are believed to be the primary contributors to NH_3 oxidation in heavily fertilized soils, it is probable that their activity plays an important role in N_2O production within agricultural systems [63]. In total, the combined emis-

sion of N_2O gas from canonical denitrification, AOBs, and AOAs are thought to make up almost 70 % of the total N_2O emissions [61].

3.4 Nitrification inhibitors

To address the issue of nitrogen loss from fertilizers and subsequently nitrogen pollution, nitrification inhibitors (NIs) have been employed for several decades. NIs are chemical compounds that regulate the activity of nitrifying organisms by inhibiting nitrification and therefore decreasing nitrifying activity. Their main mode of action focuses on the inhibition of the key enzyme, needed for nitrification which is the ammonia monooxygenase (AMO).
The AMO belongs to a significant group of membrane monooxygenases that rely on a copper ion within their active site [64]. It is the only enzyme shared among all three primary categories of ammonia oxidizers—AOAs, AOBs, and comammox but varies significantly between AOBs and AOAs [65]. The AMO of AOBs consists of three subunits (*amoA*, *amoB*, *amoC*) while the AOA's AMO is a heterohexameric enzyme containing *amoA*, *amoB*, *amoC*, *amoX*, *amoY*, *amoZ* subunits [66]. Possibly due to these structural differences, nitrification inhibitors seem to have differentiating effects and efficiencies on AOA, AOB, and comammox [67]. Hence, there are distinct inhibitors that selectively target either AOA, AOB, or comammox without exerting significant effects on the others.
As a member of the monooxygenase family, AMO has a broad substrate range [68]. Consequently, these substrates can act as competitors in NH_3 oxidation. Nevertheless, as the activation of the AMO requires two electrons - often derived from the oxidation of NH_2OH - the need for reducing equivalents can complicate the kinetics of alternative substrate oxidation, demanding alternative electron sources for AMO activation. This enzyme can thus be influenced by direct binding of alternative competing substrates, interruption of reducing equivalent supply, and oxidation of substrates yielding products that deactivate the AMO [68].
Another way of influencing the activity of the AMO is by interacting with its active site. Sulfur (S)-containing compounds like thiourea can form complexes with various metals. While compounds with internal carbon-sulfur double bonds (C=S) are primarily involved, those with terminal C=S bonds can chelate (bind to) the copper ions in the AMO [68]. This chelation reduces the ability of AMO to function properly, thereby inhibiting its catalytic cycle.
Substances containing acetylenic (C≡C) groups, such as 2-ethynyl pyridine and phenylacetylene (PA), also show strong inhibition of nitrification. However, acetylenic compounds with carboxyl groups (-COOH) do not inhibit nitrification. This is likely because the AMO enzyme has a lower binding affinity for charged compounds, such as those with carboxyl groups[68].
Another category of nitrification inhibitors includes heterocyclic compounds, which contain a ring structure with at least one atom that is not carbon (often nitrogen). The inhibitory effect of these compounds on nitrification depends on the number of adjacent nitrogen atoms in the ring. At least two adjacent nitrogen atoms are needed for these compounds to effectively inhibit nitrification[68].
Interestingly, significant parallels have been identified between AMO and methane monooxygenase (MMO), which carries out the oxidation of CH_4 in methanotrophic bacteria. Especially the particulate methane monooxygenase (pMMO) shares a nucleotide similarity of up to 70%

with the AMO of AOAs. This is particularly intriguing as the amino acid identity between the AOB and AOA AMO is only 40% [69, 70]. This similarity enables both enzymes to initiate the oxidation of either NH_3 or CH_4 [71]. Influencing the nitrogen cycle by blocking the AMO could therefore also play a significant part in altering the carbon cycle by mitigating the oxidation of CH_4 [72, 71, 73]

Although, the main path for inhibiting nitrification is based on the functionality of the AMO, some NIs, belonging to the class of polyphenolics, don't directly interact with the AMO but influence the N availability by increasing N immobilization and decreasing N mineralization, meaning that the amount of reactive nitrogen being incorporated by heterotrophic bacteria increases while less NH_4^+ is produced via mineralization [74, 75]. Additionally, phenolic compounds can be used as a carbon source for heterotrophic growth, increasing the abundance of heterotrophic microbes, concurrently increasing their demand for N [75, 76]. Typically, the carbon content of the soil plays a pivotal role, either constraining or facilitating heterotrophic growth. These, in turn, can outcompete nitrifiers for the available NH_4^+, given the higher affinity of heterotrophs for this substrate [77].
Additionally, some compounds (for instance phenolic compounds) can act as NO scavengers, therefore, disturbing the formation of necessary intermediates. Lancaster et al., (2018) suggests that this inhibitory effect is stronger on AOA as AOB have a faster enzymatic process and, therefore don't accumulate NO [78]. Compounds, scavenging NO, might therefore have a selective inhibitory effect on AOA.

3.4.1 Synthetic nitrification inhibitors (SNIs)

Commonly used NIs are all part of the synthetic nitrification inhibitors (SNIs) group, including nitrapyrin, dicyandiamide (DCD), 2-amino-4-chloro-6-methylpyrimidine, and 3,4-dimethyl pyrazole phosphate (DMPP) [67, 79, 80]. DCD, DMPP, and nitrapyrin interact with the copper in the active site of the amoB subunit [81, 68]. Nitrapyrin can also be used as an alternative substrate for the AMO, producing a chemical compound that irreversibly inactivates the AMO [82]. While SNIs do enhance nitrification use efficiency (NUE), they often present challenges such as increased costs, degradation concerns, environmental pollution, and potential risks of entering the human food chain [83]. Additionally, due to their synthetic origin, they cannot be used in organic agriculture.

3.4.2 Biological nitrification inhibitors (BNIs)

As a sustainable and natural alternative BNIs are closely studied at the moment. The term BNI refers to compounds, primarily root exudates, derived from biological sources like plants, that can inhibit nitrification[46]. Inhibiting nitrification has long been beneficial for plants as it provides them with the option to actively influence the nutrient availability around them. Especially in ecosystems, that lack high amounts of N, and are severely impacted by factors like fire, seasonal rainfall, and nutrient scarcity BNIs may facilitate better nitrogen conservation [84]. Specifically, BNIs are thought to help these ecosystems become more nitrogen-efficient and maintain higher levels of primary productivity, as ammonium is less likely to leach compared to nitrate

and is not lost through denitrification. Ammonium and nitrate can both be used by plants but maintaining a higher concentration of reactive nitrogen in the form of NH_4^+ in the surrounding soil is in most cases beneficial for plants. Most plants exhibit a preference for absorbing NH_4^+ over NO_3^- at micromolar concentrations as the uptake of NH_4^+ is associated with lower energy input compared to NO_3^-– [85, 86]. By slowing down nitrification and retaining nitrogen as NH_4^+, plants can significantly enhance nitrogen use efficiency as less reactive N is lost through leaching [87]. Additionally, these exudates are believed to maintain low nitrifying community abundances in natural systems compared to agricultural sites.

BNIs have been found in numerous plants like *Sorghum bicolor* [88], *Brachiaria humidocola*[89], *Oryza sativa*[90], *Triticum aestivum*[91] and *Leymus racemosus*[92]. The majority of BNIs appear to inhibit both AMO and HAO activity, indicating a broad and nonspecific mode of action[46]. In general, these BNIs consist of low molecular weight compounds like phenolic substances or other secondary metabolites[93]. They can be differentiated between hydrophilic, for instance, MHPP, and hydrophobic compounds. This trait also influences where the BNIs accumulate concerning their point of origin as well as the root systems. Hydrophobic substances remain close to the roots while hydrophilic substances may be transported by rainwater and can therefore leave the rhizosphere, thus potentially having a more widespread effect [94, 93].
As most of the root exudates are charged, diffusion as a form of releasing the BNIs is thought to be irrelevant. On the other side, it seems to be an active and strictly regulated process, closely coupled to the presence and amount of NH_4^+ [95].

3.4.3 Aims and Hypothesis

My master's thesis aims to look at 3 different BNIs (Table1) and test them on their potential to inhibit nitrification in agricultural soil from Linz. I will assess their inhibitory effect by defining the effective concentration 50 value (EC50) for each compound by testing different concentrations and evaluating the percentage of inhibition for each respective concentration. The BNIs tested are Methyl 3-(4-Hydroxyphenyl)Propionate (MHPP3.4.4), Methyl 3-(4-hydroxyphenyl)acrylate (MHPA3.4.5) and DL-p-Mentha-1,8-dien, 4-Isopropenyl-1-methylcyclohexen (limonene3.4.6). As control groups, I used the SNIs phenylacetylen which achieves total nitrification inhibition, and octyne which only inhibits bacterial nitrifiers (AOB, Comammox). I will compare this data to previous experiments of my colleague Paula Rojas [96], which tested the respective components on soil from Wieselburg and Marchfeld. With her additional data, I will try to find patterns that explain differences in inhibitor efficiency. In this sense, I will look deeper into soil characteristics and possible correlations between soil parameters and varying BNI efficiencies. Additionally, I aim to make a community analysis of the tested soil, by DNA sequencing to assess the community composition. I will take a closer look at the whole community, identifying dominant clades, analyzing the diversity and evenness, and closely examining the nitrifying community and its participants. In addition, I will perform qPCR for AOB, AOA, and comammox *amoA* genes to assess the abundance of each clade and correlate it to their activity by performing an RT qPCR.

Table 1: list of nitrification inhibitors used in this experiment.

	full name	type	mode of action	target
BNI	MHPP (Methyl 3-(4-Hydroxyphenyl)Propionate)	Phenylpropanoid	unknown	AMO
	Limonene (DL-p-Mentha-1,8-dien, 4-Isopropenyl-1-methylcyclohexen)	Phenylpropanoid	unknown	AMO
	MHPA (Methyl 3-(4-hydroxyphenyl)acrylate)	Mono-terpene	unknown	unknown
SNI	Phenylacetylen	Alkyne	non-competitve inhibitor	AMO
	1-octyne	Alkyne	competititve inhibitor	AMO

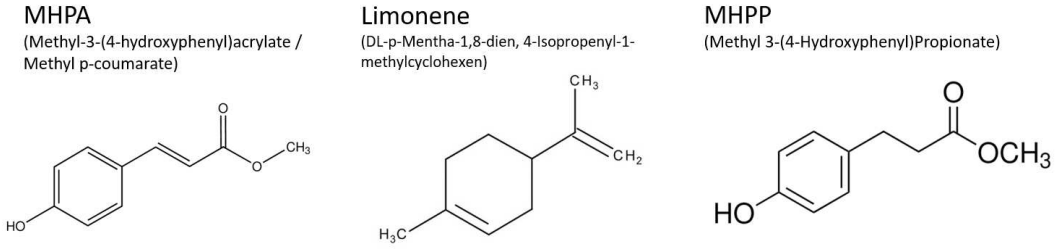

Figure 2: chemical structure of BNIs used in this experiment.

3.4.4 MHPP (Methyl 3-(4-Hydroxyphenyl)Propionate)

Is a root exudate from *Sorghum bicolor*. Its main mechanism of action is interfering with the AMO and by inhibiting NO_2^- oxidation by NOB [88]. Its release is interlinked with a low pH and the presence of high NH_4^+ concentrations [88]. In addition to its inhibitory function, MHPP also stimulates root growth and branching, providing an additional benefit for the plant [97].

3.4.5 MHPA (Methyl 3-(4-hydroxyphenyl)acrylate)

Is a root exudate from *Brachiaria humidicola*, which is a tropical grass from South America [98]. Studies suggested an inhibitory effect of *B. humidicola* as grass fields containing *B. humidicola* show lower NO_3^- concentrations than other grass fields [99, 100].

3.4.6 DL-Limonene (DL-p-Mentha-1,8-dien, 4-Isopropenyl-1-methylcyclohexen)

Is a phenolic compound and belongs to the group of terpenoids [101]. The first proposal of monoterpenes having an inhibitory effect was based on the chemical similarity of terpenes to known NIs that have an inhibitory effect on AMO [102].

4 Materials and methods

4.1 EC50 experiment

4.1.1 Sample collection and processing

Soil samples were collected in Ritzlhof, Linz, Austria (48°18N 14°25E) on 09.05.2023. The soils are part of a long-time experiment of the Austrian Agency for Health and Food Safety (AGES) [103] and have formerly been described as a loamy silt Cambisol (17.4 % clay, 69 % silt, and 13.6 % sand), with a pH of around 6.8 [104, 105, 106]. During sample collection, the conditions were sunny and dry and the temperature was around 12°C. We collected 4 different soil samples (4a, 4b, 4c, 4d) at a depth of approximately 10 cm. They all received the same treatment (120 kg N ha^{-1} $year^{-1}$) and were therefore used as biological replicates. The soils were then sieved with a 2 mm sieve and stored at 4°C until further processing.

4.1.2 Soil characteristics

Soil water content was determined by drying 5 g of soil at 60°C for 48 hours. The soil was weighed before and after drying and the difference in weight refers to the water content in the soil. The dried and ground samples were then analyzed for total carbon (C) and total nitrogen (N) content by using an EA-IRMS (EA 1110, CE Instruments, Italy), coupled to a Finnigan MAT Delta Plus IRMS (Thermo Fisher Scientific, MA, USA). Soil pH was measured by dissolving the soil in water with pH electrodes at a 1:5 soil-to-water ratio. The contents of $CaCO_3$, EDTA-extractable iron, manganese, copper, zinc, and cation exchange capacity (CEC) were determined by the Austrian Agency for Health and Food Safety (AGES) following the standard protocols ÖNORM L1084, L1098, and L1086-1.

4.1.3 Experimental setup

A 5 g soil sample was placed in a 125 ml Wheaton bottle. Subsequently, 25 ml of autoclaved Milli-Q water and 53.5 µl of 1 M NH_4Cl (corresponding to a fertilization rate of 150 mg N kg^{-1} soil) were added. Then, 50 µl of the specific treatments listed in Table 3 were introduced. The slurries were homogenized by manually turning and shaking them for approximately one minute. Initial samples were then collected (T0). Each treatment was done in quadruplets.

4.1.4 Sampling procedure

1 ml of slurry was withdrawn with a syringe (10 ml) (Table10) and put in a 2 ml sample vial. Then the samples were centrifuged for 3 min at 18200 rcf. The supernatant was then transferred to a new sample vial and stored at -20°C. The sample time points are shown in Table4 and Table5. As an increase in the nitrification rate, indicative of growth, was observed in control treatments after 46 hours of incubation, only time points until 46 hours are considered for data analysis. Time points after 47 hours will be excluded.

Table 2: Soil characteristics for Linz, Marchfeld and Wieselburg. Data for Marchfeld and Wieselburg was collected previously and is describes in Rojas et al. 2023 [96].

	Linz		Wieselburg		Marchfeld	
	mean	Stdv	mean	Stdv	mean	Stdv
total C	14.01	0.00	8.40	0.00	23.23	0.00
pH	6.64	0.24	7.57	0.05	5.63	0.13
$CaCO_3$ %	0.00	0.00	12.00	0.97	0.00	0.00
Sand %	16.48	1.38	30.28	2.91	9.45	0.86
Silt %	67.63	1.19	45.58	2.72	71.15	1.25
Clay %	15.90	0.24	24.15	0.90	19.40	0.82
Iron (mg/kg)	643.50	118.83	65.50	4.77	480.50	30.64
Manganese (mg/kg)	478.75	20.50	149.75	39.41	375.50	12.99
Copper (mg/kg)	9.15	1.34	5.95	0.54	4.70	0.07
Zinc(mg/kg)	9.73	2.44	2.60	0.43	2.43	0.16
Calcium (cmolc/kg*)	13.42	1.49	24.69	0.67	7.06	0.54
Magnesium (cmolc/kg*)	1.20	0.21	1.57	0.07	1.04	0.15
Potassium (cmolc/kg*)	0.40	0.04	0.74	0.04	0.40	0.06
Sodium (cmolc/kg*)	0.02	0.00	0.02	0.00	0.03	0.00
Aluminium (cmolc/kg*)	0.01	0.01	0.00	0.00	0.07	0.03
Manganese (cmolc/kg*)	0.03	0.02	0.00	0.00	0.20	0.01
CEC**	15.07	1.37	27.02	0.71	8.80	0.63

*cmolc/kg = centimol positive charge per kg of soil; **CEC = cation exchange capacity

4.1.5 NO_2^-/ NO_3^- measurements

For the quantification of NO_2^-/NO_3^- concentrations for each sampling point, the Griess reaction was used [107, 108, 109]. Standard solutions for NO_2^- and NO_3^- were prepared by preparing a standard series ranging from 1 mM to 0.001 mM. 100 µl of Milli-Q (MQ) water was put into each well of a deep well plate. Subsequently, 50 µl of the standard solution was added in triplicates, along with 50 µl of the sample. Following this, 750 µl of Griess reagent was added to each well. Further on, two times 200 µl from each well was transferred to two new 96-well plates as technical duplicates. Before the transfer, samples were homogenized by gently pipetting up and down to ensure thorough mixing with the Griess reagent. The plates were then subjected to measurement using the TECAN Infinite Pro Nano 200i plate reader, and the absorbance was recorded at a wavelength of 540 nm to determine NO_2^- concentrations in the samples.
After that, 35 µl of VCl_3 solution was added to each well and was incubated for 2 hours at 46°C to convert the NO_3^- present in the samples to NO_2^-. The plates were then again measured as described above. By subtracting the values from the first measurement from the second measurement (ΔNO_2^-), the amount of NO_3^- was determined. When assessing the EC50 value, it was crucial to only consider the time points that indicate activity without significant growth. Including growth rates in the EC50 calculation could introduce distortions from other growth-influencing factors such as nutrient availability, temperature, and pH. The EC50 measurement

Table 3: Treatments and final concentrations concentrations.

treatment	concentration (µM)
MQ	
DMSO	1000
Pheylacetylen	1000
octyne	100
MHPP	1500
	1000
	750
	500
	150
Limonene	1500
	600
	250
	75
	25
MHPA	1500
	750
	200
	75
	25

aims to isolate the compound's effect without being affected by external growth factors. For both experiments, growth was observed after approximately 45 hours. For experiment one, only time points T0, T1, T2, T3, and T4 (a total of 46 hours - Table4) are considered. Due to a missed second measurement in experiment two, only time points T0 to T3 (a total of 47 hours - Table5) are included in the EC50 calculations.

4.1.6 Data processing

The initial measurements obtained from the TECAN were multiplied by the volume of the slurry in the bottle for each time point to yield µmol. At each sampling point, 1 ml was withdrawn from the slurry, resulting in varying final volumes of slurry for each time point. Subsequently, this value was divided by the soil's dry weight to obtain µmol g^{-1} of dry weight (DW). Finally, the result was multiplied by the molar mass of nitrogen of $NO_3{}^-$, which is 14.01 g, to yield $NO_3{}^-$ µg g^{-1} DW soil. The phenylacetylene control was utilized to account for heterotrophic $NO_3{}^-$ consumption and was included in all treatments to resemble 0 nitrification. Due to irregular behavior observed in soil replicate D, it was excluded from the data analysis.

To determine the EC50 value, the $NO_3{}^-$ production for each compound at each concentration and timepoint was calculated. Pheylacetylen showed no $NO_3{}^-$ accumulation but consumption, mirroring the DMSO effect on the heterotrophic growth. The rate for each timepoint was then calculated by dividing the $NO_3{}^-$ production at that specific timepoint by the time elapsed

Table 4: sampling points for experiment 1.

Date	sampling time	time (h)	name
05.06.2023	11:30	0	T0
05.06.2023	17:30	6	T1
06.06.2023	09:00	22	T2
06.06.2023	16:00	29	T3
07.06.2023	09:00	46	T4

Table 5: sampling points for experiment 2.

Date	sampling time	time (h)	name
20.06.2023	10:30	0	T0
21.06.2023	09:30	23	T1
21.06.2023	16:30	30	T2
22.06.2023	09:30	47	T3

since T0 ($T = Tn - T0$). This rate was subsequently compared to the DMSO control, representing a 100% Nitrification rate.

Using these values, the percentage of inhibition was assessed using the Excel add-in Solver (version 3.0.0.1), considering the Sumsquare and Hill coefficient.

4.2 Microbial community analysis

4.2.1 DNA/RNA extraction

To analyze the community composition, approximately 0.250 g of soil samples were collected in duplicate and stored at -80°C in DNA Lysis Matrix E tubes for subsequent use. DNA and RNA extraction were performed using the ZymoBIOMICS DNA/RNA Miniprep Kit. DNAse 1 reaction mix was prepared by adding 5 µl of DNAse 1 to 75 µl of DNA digestion buffer. Buffer preparation consisted of adding 96 µl of ethanol (100 %) to the 24 ml of DNA/RNA wash buffer. Samples were initially prepared by adding 750 µl of DNA/RNA shield to the tubes, followed by bead beating for 40 seconds at 6.0 m/s. Subsequently, the samples were centrifuged for 6 minutes at 12,851 rcf. The supernatant (400 µl) was then transferred to new DNA/RNA-free sample vials, where 400 µl of DNA/RNA Lysis buffer was added and vortexed. After transferring the samples to spin-away filters in new collection tubes and centrifugation(30 sec; 12,851 rcf) , yellow filters containing DNA were isolated and temporarily stored on ice.

For RNA extraction, 750 µl of ethanol (100%) was added to the flow-through, mixed, and then transferred to green spin-away filters. Following two centrifugation (30 sec; 12,851 rcf) steps to remove flow-through, 400 µl of DNA/RNA Wash Buffer was added and centrifuged (30 sec; 12,851 rcf). Next, 80 µl of DNAse1 reaction mix was directly added to the column and incubated for 15 minutes at room temperature.

Subsequently, 400 µl of DNA/RNA prep buffer was added to both RNA- and DNA-containing

filters, followed by centrifugation(30 sec; 12,851 rcf) to discard the flow-through. This process was repeated with 700 µl of DNA/RNA wash buffer and again with 400 µl of DNA/RNA wash buffer, followed by centrifugation for 2 minutes at 12,851 rcf. The column was then placed into a new collection tube, and 100 µl of DNAse-free water was added directly to the columns and incubated for 5 minutes.

Meanwhile, Zymo-Spin III-HRC filters were prepared by adding 600 µl of prep solution and centrifuging for 3 minutes at 12,851 rcf. The samples were then centrifuged(30 sec; 12,851 rcf) again, and the flow-through, now containing DNA/RNA, was placed on the prepared HRC filters and centrifuged at maximum speed for 3 minutes. The DNA was stored at -20°C, while the RNA was stored at -80°C.
The final amount of DNA for each sample was measured with Qubit 4.0 Fluorometer (Thermo Fisher Scientific) using the Qubit dsDNA HS Assay Kit.

4.2.2 RNA purification

To ascertain the presence of residual DNA in the RNA samples, a 16S rRNA gene-targeted PCR assay was performed. The master mix was prepared as described in section 4.4. For the positive control, a concentrated sample of *N. inopinata* was utilized, while the negative control consisted of PCR water.

The cycling conditions can be found in section 4.3. The gel was produced as described in section 4.4. The gel was then run at 120 V for 40 minutes.
As DNA was still left in the samples an additional purification step was conducted using the ezDNase protocol. A master mix was prepared, consisting of 4 µl 10x ezDNase buffer, 4 µl ezDNase enzyme, and 4 µl DNase free water. 2 µl of this master mix was added to 8 µl of RNA sample. The samples were then mixed gently and spun down. Subsequently, they were incubated for 2 minutes at 37°C. To check if there was still DNA left after this additional treatment another 16S rRNA gene-targeted PCR was performed as described above. Due to ongoing DNA contamination, an additional amount of 1 µl of ezDNase was added to the samples and incubated for 2 minutes at 37°C. Another 16S rRNA gene-targeted PCR was performed as described above.

4.2.3 qPCR

QPCR was done using primers for 16S rRNA, archaeal *amoA*, bacterial *amoA*, and comammox *amoA* genes. Specific primers are listed in Table6. The master mixes were prepared as described in section 4.4. The 16S rRNA gene qPCR was done to quantify the total microbial community and define the percentage of the whole community comprising of nitrifiers. Cycling conditions can be found in section 4.3, mastermix preparation is described in section 4.4.
For analyzing the qPCR data, copies μl^{-1} were calculated and averaged for each soil specifically. This value was then divided by the amount of DNA present in each sample to get to copies μg^{-1} of DNA. Additionally, the copies μl^{-1} were multiplied with the final volume of the DNA extraction (100 µl) and divided by the dry weight of each sample to get to copies g^{-1} soil.

Table 6: Primers used for qPCR analysis. References: 1F/2R [110], 104F/616R [111], comB-244F/comB-659R [36], 515F [112], 806R [113]

	Primer F	sequence F	Primer R	sequence R
AOB	1F	GGGGTTTCTACTGGTGGT	2R	CCCCTCKGSAAAGCCTTCTTC
AOA	104F	GCAGGAGACTAYATHTTCTA	616R	GCCATCCATCTRTADGTCCA
ComB	comaB-244F	TAYTTCTGGACRTTYTA	comaB-659R	ARATCCARACDGTGTG
16S rRNA	515F	GTGYCAGCMGCCGCGGTAA	806R	GGACTACNVGGGTWTCTAAT

4.2.4 RT-qPCR

To evaluate the activity of each clade (AOA, AOB, ComA, and ComB), reverse transcription qPCR (RT-qPCR) was conducted using specific primers targeting the *amoA* gene of each clade. The Luna® Universal One-Step RT-qPCR Kit was employed for this purpose. Purified RNA was diluted at a ratio of 1:10, and 2 µl of the resulting template were added to the master mix as described in section 4.4. Cycling conditions can be found in section 4.3. Given the presence of residual DNA in the RNA template, it was imperative to correct for this during analysis. To address this concern, an additional master mix was prepared as described in section 4.4, omitting the enzyme mix to prevent cDNA synthesis from RNA. The results obtained from this second RT-qPCR provided insight into the signal attributable to residual DNA, which was subsequently subtracted from the primary RT-qPCR data to yield accurate activity data.

4.2.5 Phylogenetic analysis of soil microbiome

Amplification and sequencing of the *amoA* and the 16S rRNA genes were conducted at the Joint Microbiome Facility of the Medical University of Vienna and the University of Vienna (JMF). The primers used are shown in Table6. Target gene amplification and sample barcoding were executed using a two-step PCR protocol, consisting of an initial PCR for target amplification and an additional Barcoding-PCR reaction[114]. Additionally, a dual barcoding approach was used to minimize sequencing errors like mismatches or "crosstalk" which can be quite common in single-barcoding approaches [114]. The sequencing process was performed on the Illumina MiSeq platform. The raw data obtained from sequencing were processed through the FASTQ workflow in Basespace (Illumina) using the default settings. Amplicon sequence variants (ASVs) were then inferred using the DADA2 pipeline following the recommended procedures [115]. The taxonomic classification for prokaryotic 16S rRNA gene amplicons was conducted using the SILVA database [116].
For analyzing the microbial community and its phylogenetic composition, the total ASV counts were added up, and the relative abundance for each phylum and class was evaluated by calculating the percentage of their counts relative to the overall soil counts. Furthermore, the relative abundance of each nitrifier clade (AOA, AOB, ComA, ComB) was determined using the same method. Additionally, this relative data was combined with the 16S rRNA gene qPCR data to determine absolute numbers by multiplying the percentage of each respective group with the total abundance of 16S rRNA gene qPCR copies. ASVs were sorted by abundance and those, making up $\geq$ 2% of the whole community in at least one soil replicate were included in data analysis and visualization. On a higher phylogenetic level, only groups with an overall share

$\geq 1\%$ of the whole community are shown.
The *amoA* gene qPCR data underwent analysis by multiplying the average copies μl^{-1} with the total volume of the DNA sample (100 µl). Subsequently, this product was divided by each soil's dry weight (DW) to obtain copies g^{-1} DW soil. Given that AOA and Comammox typically possess one copy of the AMO enzyme, whereas AOB possesses an average of 2-3 copies, the data required normalization by dividing the AOB counts by 2.5.

To assess the diversity of microbial communities across different plots, we calculated alpha diversity indices, including species richness, evenness, and the Shannon diversity index for each functional group (ComB, AOA, AOB) across four plots (A, B, C, D). Species richness was calculated by summing the number of unique taxa (ASVs) present in each plot. Richness for each plot was determined by counting the number of ASVs with non-zero abundance values. Overall richness across all plots was calculated by summing the number of ASVs present in any of the plots. Evenness, which measures the uniformity of taxa distribution within each plot, was calculated using Pielou's evenness index. This index was derived by dividing the Shannon diversity index by the natural logarithm of species richness. The Shannon diversity index was computed for each plot individually, as well as for the overall community by summing the abundance data across all plots. For each plot, the number of taxa (richness), the Shannon diversity index, and evenness were calculated using the vegan package in R.

4.3 Cycling conditions

Table 7: Cycling conditions for PCR, qPCR, and RT qPCR

	Primers	cycle step	temperature (°C)	duration	cycles
16S rRNA PCR	515F 806R	initial denaturation	94	4 min	
		denaturation	94	30 s	40
		annealing	52	30 s	
		elongation	72	1 min	
		final elongation	72	15 min	
16S rRNA qPCR	515F 806R	initial denaturation	95	5 min	
		denaturation	95	30 s	
		annealing	52	30 s	
		elongation	72	30 s	40
		final elongation	72	2 min	
		Melting curve analysis			
AOB *amoA*	1F 2R	initial denaturation	95	5 min	
		denaturation	94	1 min	
		annealing	60	1.5 min	
		elongation	72	1.5 min	40
		Melting curve analysis			
ComB *amoA*	comaB_244F comaB_659R	initial denaturation	95	3 min	
		denaturation	95	30 s	
		annealing	52	45 s	
		elongation	72	1 min	40
		Melting curve			
ComA *amoA*	comaA_244F comaA_659R	initial denaturation	95	3 min	
		denaturation	95	30 s	
		annealing	52	45 s	
		elongation	72	1 min	40
		Melting curve analysis			
RT qPCR		reverse transcription	55	10 min	
		initial denaturation	95	1 min	
		denaturation	95	10 s	
		elongation	60	30 s	40
		Melting curve analysis			

4.4 Preparation of buffers/solutions

Table 8: Preparation of Mastermixes (MM)

		for 1 reaction (µM)
MM 16S rRNA gene qPCR	PCR-MQ	10
	Reaction buffer SYBR Green	10
	Primer 515F (50 µM)	0.1
	Primer 806R (50 µM)	0.1
	Taq DNA Polymerase	0.25
	Template	2
MM MM for AOB/AOA amoA gene qPCR	PCR-MQ	10
	Reaction buffer SYBR Green	10
	Primer F (10 µM)	0.5
	Primer R (10 µM)	0.5
	Taq DNA Polymerase	0.5
	Template	2
MM for RT-qPCR	Nuclease free water	14.6
	Luna WartStart RT Enzyme mix (20X)	1
	Luna universal One-Step reaction mix (2x)	10
	Primer F (10 µM)	0.8
	Primer R (10 µM)	0.8
	Template	2
MM for 16S PCR	PCR-MQ	17.5
	10x DreamTaq Buffer	2.5
	Primer F (50 µM)	4
	Primer R (50 µM)	4
	BSA	2
	Taq DNA-Polymerase	2
	Template	
MM for RT qPCR	Reaction mix	10
	Enzyme mix	1
	F-Primer (10 µM)	0.8
	R-Primer (10 \textmu M)	0.8
	PCR-MQ	7.4
MM for checking for residual DNA (RT qPCR)	Reaction mix	10
	Enzyme mix	-
	F-Primer (10 µM)	0.8
	R-Primer (10 µM)	0.8
	PCR-MQ	8.4

4.4.1 PCR - gel analysis

The gel was produced by mixing 100 ml of 1x TBE buffer and 1 g of agarose. The mixture was heated up until the agarose was dissolved completely. The mix was then cooled down under running water for 1 minute. 1 µl of GelRed Nucleic Acid Gel Stain was added and mixed, then the liquid gel was poured and left to harden.

4.5 Instruments used in this experiment

Table 9

Instruments	
MQ-Machine	Milli-Q QPOD with Millipak Gold (0.22uM filter)
Shaker	LAUDA VS30 0
pH Meter	Hanna HI 5522 v1.0
Centrifuge	eppendorf Centrifuge 5804R with PL099 insert
PCR Cycler	BIO-RAD T100 Thermal Cycler
QPCR Cycler	BIO-RAD CFX96^{TM} Real-Time System
Pipet boy	Integra Pipetboy 2
scale (inhibitors and chemicals)	sartorius - QUINTIX 124 - 1S
Multi-dispenser pipette	eppendorf - Multipipette E3
Multi-channel pipette	eppendorf Research plus Multichannel
Gel-Elektrophorese	biotechservice blue bsb11
Plate Reader	TECAN Infinite M200 Pro Nano^{+} with Tecan-i-control 2.0 programm
Pipettes	eppendorf Reserach plus 2.5µl, 10 µl, 20 µl, 200 µl, 1000 µl
Vortex	Vortex-Genie 2
Incubator	memmert - D39872
PCR Gel reader	BIO-RAD Geld-Doc^{TM} with ImageLab^{TM} 5.2

4.6 Materials used in this experiment

Table 10

Material	additional information
wheaton bottles 125 ml	
black caps for wheaton bottels (P03537 H - NNBC 7 G) with rubber septa	
serological pipette 25 ml	avantor 612 - 3698 disposable serological pipette
Syringe for Octyne	Omnifix 60 ml. luer lock - 4617509F
Epi-cups 2.2 ml	Greiner Bio-One 623201
Epi-cups 1.5 ml	Greiner Bio-One 616201
Syringe for sampling	Omnifix F-luer Solo-9161406V
Syringe for overpressuring bottle	30 ml Omnifix gastight, luer-lock - 46173047
Needles for overpressuring	Stericon BRAUN, 0.80 x 40 mm - 4657527
Pipette tips	1000 ul Biotix 300 ul Biotix 200 ul Biotix 20 ul Biotix
needles for sampling	Safe-lock BROWN Sterican - 0.90 x 40 mm - 46700505
Deepwell plate	96 Deepwellplate BIOLOGIX round bottom 1 ml 02-2010-50
96 well microplates	96-well U-bottom - 650261
Combitips for multidispenser pipette	Combitips advanced 1 ml , 0.5 ml, 5 ml
Gloves	ecoSHIELD Eco Nitrile PF 250 S-62 5122

5 Results

5.1 Assessment of BNI inhibitory potential

As shown in Figure 3.a, the control treatments in the MHPA experiment exhibited steady increases in NO_3^- concentration over time, with final concentrations of 42.9 ± 16.3 µmol g^{-1}(MQ) and 35.8 ± 9.7 µmol g^{-1} (DMSO) after 46 hours of incubation. NO_3^- accumulation in the presence of octyne displayed a final concentration of 10.4 ± 4.3 µmol g^{-1} at T3. Increasing concentrations of MHPA showed varying effects on NO_3^- accumulation. Higher concentrations (1.5 mM and 0;75 mM) led to significant decreases in NO_3^- production with a final concentration of 3.6 ± 2.3 and 8.1 ± 3.9 µmol g^{-1}. Lower concentrations (0.2 mM, 0.075 mM, 0.025 mM) resulted in significant NO_3^- concentration increases over time, ranging from 21.3 ± 4.3, 25.1 ± 5.8 to 28.4 ± 5.7 µmol g^{-1} after 46 hours.
Additionally, the average inhibition potential was assessed and normalized with DMSO representing 100% of nitrification potential as shown in Figure 3.b. We already see an inhibitory potential when comparing the DMSO control to the MQ control which exhibits 13.7 ± 6 % more nitrification. Octyne, a specific inhibitor for nitrifying bacteria (AOB, comammox) exhibits a strong inhibitory effect as only 6.7 ± 7.9 % nitrification potential was achieved. MHPA in its highest concentrations (1.5 mM and 0.75 mM) shows nitrification potential of -13 ± 10.4 % and 3 ± 12.5 %. Concentrations ranging from 0.2 mM to 0.025 mM exhibited a plateau with 0.2 mM showing 48.5 ± 16.2 %, 0.075 mM showing 53.6 ± 12.7 %, and the lowest concentration showing 57 ± 9.3 % of possible nitrification.
As depicted in Figure 3.(c,e), the control treatments in the MHPP and limonene experiment displayed consistent increases in NO_3^- accumulation over time, reaching final concentrations of 36.3 ± 18.6 µmol g^{-1} (MQ) and 20.1 ± 15.7 µmol g^{-1} (DMSO) after 46 hours of incubation. The presence of octyne yielded a final concentration of 1.2 ± 1.2 µmol g^{-1} at T3. The average rate was evaluated and normalized using DMSO as the reference representing 100 % nitrification potential, as illustrated in Figure 3.d,f. A notable inhibitory potential is evident when comparing the DMSO control to the MQ control, which exhibits 16.2 ± 14.6 % more nitrification. The control treated with octyne showed a nitrification potential of -15.3 ± 7.7 %.
The effects of increasing concentrations of MHPP on NO_3^- accumulation varied (Figure 3.c). Higher concentrations (1.5 mM and 1 mM) led to significant decreases in NO_3^- production, resulting in final concentrations of -3.9 ± 2.2 and 1.4 ± 7.9 µmol g^{-1}, respectively, mirroring the effects observed with octyne treatment and depicting NO_3^- consumption. The 0.75 mM concentration showed a final NO_3^- concentration of 8.7 ± 10.7 µmol g^{-1}. Lower concentrations, such as 0.5 mM and 0.15 mM, already exhibited mild inhibitory effects, with NO_3^- accumulations of 18.4 ± 8.1 µmol g^{-1} and 21.6 ± 10.1 µmol g^{-1}, respectively.
Considering the percentage of nitrification potential as shown in Figure 3.d, MHPP at its highest concentrations (1.5 mM and 1 mM) exhibited similarities to the octyne control with -13.4 ± 10.1 % and -10.9 ± 17.4 %. MHPP 0.75 mM showed a nitrification potential of 8.6 ± 18.1 %. Lower concentrations of 0.5 mM and 0.15 mM already had a much lower inhibitory effect (46.2 ± 27.1 % and 66.5 ± 14.7 %).

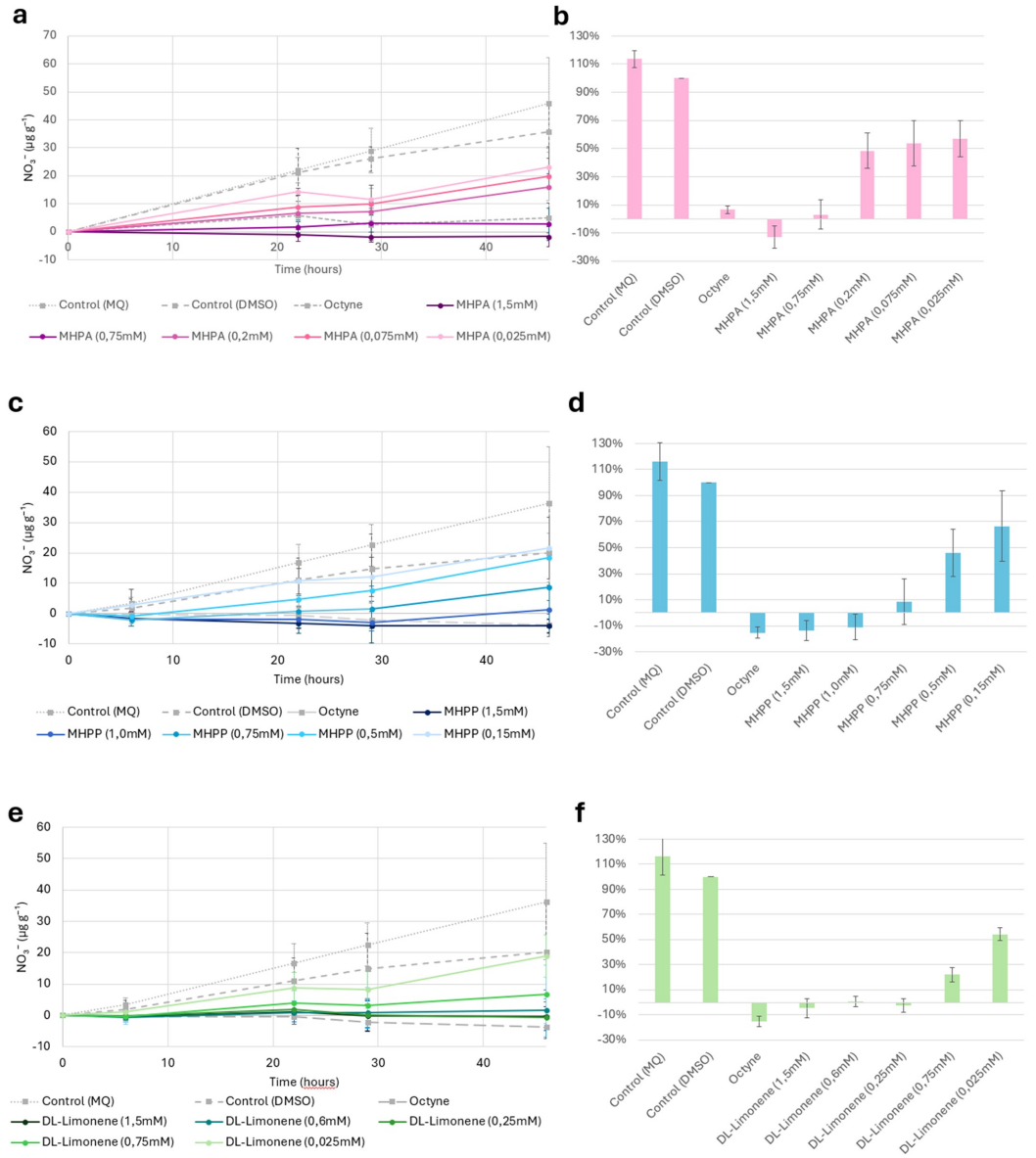

Figure 3: **(a,c,e)**These graphs illustrate the accumulation of NO_3^- over time and the impact of various inhibitors. Darker colors indicate higher inhibitor concentrations, while lighter colors indicate lower concentrations. The control groups are represented by grey lines. Graphs **(b,d,f)** display the percentage of the potential nitrification rate, normalized to DMSO, which represents a 100% nitrification rate.

Limonene showed a strong inhibitory effect at higher concentrations (1.5 mM, 0.6 mM and 0.2 mM), with NO_3^- production resulting in final concentrations of -0.5 ± 3.3, 1.6 ± 6.5 µmol g^{-1} and -0.8 ± 6.2 µmol g^{-1}, respectively (Figure 3.e). The 0.075 mM concentration yielded a final NO_3^- concentration of 6.7 ± 9.3 µmol g^{-1}, while the lowest concentration of 0.025 mM

showed a NO_3^- increase of 19 ± 6.8 µmol g^{-1}.
In terms of nitrification potential, as shown in Figure 3.f , Limonene exhibited similar effects at its highest concentrations (1.5 mM, 0.6 mM, and 0.25 mM), with values of -4.7 ± 4.1 %, 0.5 ± 5.3 %, and -2.4 ± 5.8 %, respectively. At 0.075 mM, the nitrification potential already showed higher values, reaching 22.2 ± 5.1 %. A decreased inhibitory effect was observed at its lowest concentration (0.025 mM), with a nitrification potential of 54.2 ± 17.4 %.

The EC50 values differed greatly between the different BNIs as seen in Figure 4. MHPP was least effective with a BNI of 374.9 ± 190.1 µM. The values for MHPA and Limonene were much lower as MHPA showed an EC50 of 170.5 ± 106.2 µM and Limonene 26.5 ± 11.6 µM.

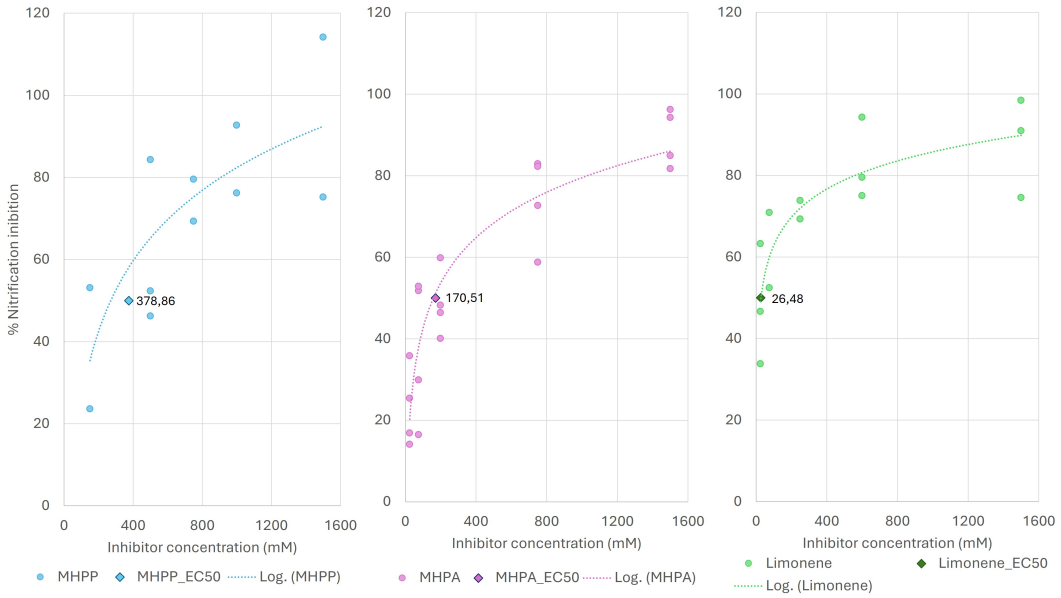

Figure 4: **EC50 values**

In the results for Marchfeld, published in Rojas et al., 2024 and as shown in Figure.5 the EC50 values were significantly higher, with MHPP exhibiting the poorest performance, showing an EC50 value of 460.3 ± 31.6 µM. MHPA and Limonene demonstrated nearly identical EC50 values, measuring 103.5 ± 10.1 µM and 102.7 ± 27.3 µM, respectively [96].

Conversely, Wieselburg displayed different patterns. MHPA had the lowest EC50 value of 34.7 ± 10.7 µM, indicating the highest potency. Limonene had an EC50 value of 96.8 ± 30.5 µM, while MHPP again showed the lowest performance with an EC50 value of 359.4 ± 18.6 µM (Figure 5)[96].

	Linz	Marchfeld	Wieselburg
MHPP	374,9 ± 190,1	460,3 ± 31,6	359,4 ± 18,6
Limonene	26,5 ± 11,6	102,7 ± 27,3	96,8 ± 30,5
MHPA	170,5 ± 106,2	103,5 ± 10,1	34,7 ± 10,7

Low High

Figure 5: EC50 values of Linz, Wieselburg and Marchfeld soil.

5.2 Correlations between EC50 values and soil physiochemical parameters

A significant correlation was observed between various soil parameters. As anticipated, the proportions of clay, silt, and sand exhibit strong intercorrelations, given their combined contribution to the soil's composition. Moreover, the soil's clay percentage shows a noteworthy correlation with the concentrations of total manganese (mg/kg) and total iron (mg/kg) within the soil. Similarly, total copper and total zinc levels also demonstrate a notable correlation. Additionally, sodium content correlates with the concentrations of dissolved manganese (cmolc/kg) and aluminum (cmolc/kg) in the soil. The soil parameters of those clusters with the lowest intercorrelation (% clay, pH, copper, sodium, total C content) to other parameters were chosen to represent this correlation cluster.

MHPP and Limonene exhibit clustering when examining the correlation between their EC50 values and the four soil parameters as seen in Figure 6(b,c). The inhibitory potential of both compounds negatively correlated with the soil's total copper concentration (R^2 = 0.96) and showed no correlation with the other parameters under investigation. MHPA's inhibitory potential exhibits an inverse relationship with pH (R^2 = 0.93), whereas the sodium content (R^2 = 0.95) and total organic C content (R^2 = 0.98) is positively associated with MHPA EC50 values (Figure 6.a)

5.3 Microbial community composition

5.3.1 Taxonomic composition of microbial communities in soil samples

The soil samples' taxonomic composition of microbial communities was analyzed through 16S rRNA gene amplicon sequencing. It revealed a diverse array of bacterial and archaeal phyla. The most abundant bacterial phylum observed was Proteobacteria, accounting for an average of 22 % of the microbial community, followed by Acidobacteriota (16.8 %), Verrumicrobiota (12

%), and Bacteriodota (10,6 %).

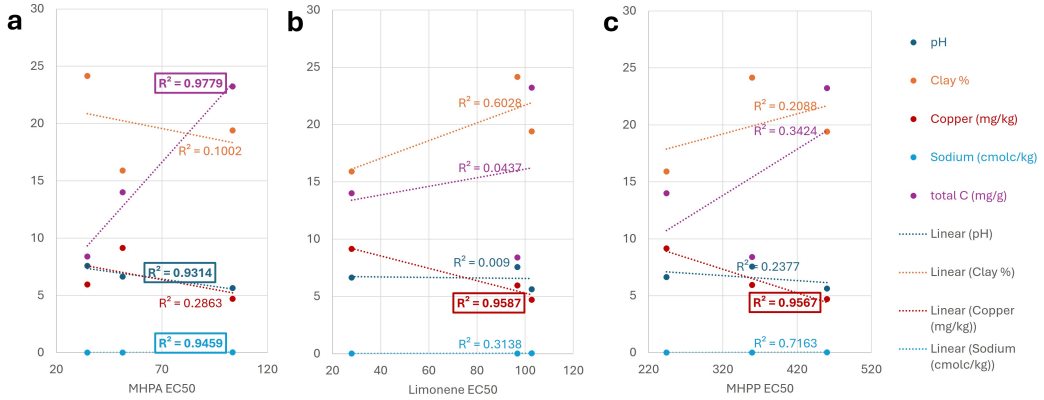

Figure 6: **EC50 soil parameter correlation** depicts the correlation of each inhibitor with soil parameter pH, %clay, copper, total organic C, and sodium content. Bold and highlighted R^2 suggests a high correlation.

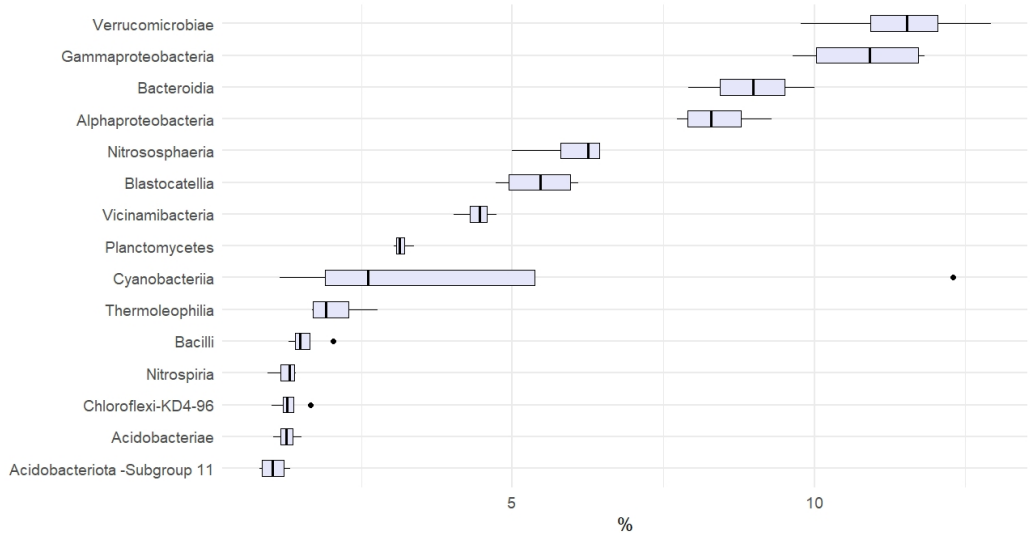

Figure 7: **Microbial community class distribution:** depicts the distribution of different classes in the microbial community of the soil. Only classes making up $\geq 1\%$ were considered.

Several other bacterial phyla were identified, albeit in lower abundance. These included Actinobacteriota (7.2 %), Crenarchaeota (6.8 %) and Cyanobacteria (5.3 %). Additionally, Planctomycetota (4.2 %), Chloroflexi (3.5%), and Firmicutes (2.1 %) were present at relatively

minor levels. Archaea were only represented by one phyla which is Crenarchaeota and accounted for 6.8 % of the total microbial community.
At the class level, the four most prevalent clades collectively constitute nearly 40 % of the entire community (39.6 %) (Figure7). These include Verrumicrobiaea (11.4 %), Gammaproteobacteria (10.8 %), Bacteroidia (9 %) and Alphaproteobacteria (8.4 %).

Organisms capable of nitrification, including representatives from Proteobacteria, Crenarchaetoa, and Nitrospirota, constituted 8.64% of the total microbial community. AOA comprised 6 % of the whole community while the remaining 2.7 % comprised AOB and *Nitrospira* (Figure 8). However, it is crucial to note that distinguishing comammox bacteria from other members of the *Nitrospira* genus based solely on 16S rRNA gene sequences is challenging. All currently known comammox organisms belong to *Nitrospira sublineage II*, which also includes canonical nitrite-oxidizing bacteria (NOB) that do not possess the genes required for ammonia oxidation [7, 8, 117]. As highlighted by Pjevac et al. (2017)[36], 16S rRNA gene sequences therefore cannot reliably differentiate between comammox *Nitrospira* and other representatives of this *Nitrospira* lineage that are not able to perform the whole nitrification process. Any comammox predictions related to *Nitrospira* based on 16S rRNA sequences, and therefore assumptions should not be considered definitive without further verification through specific molecular markers or functional gene analysis. Analyzing only the nitrifying community, *Nitrosophaeraceae*, representing AOA, comprised the majority at 68.8 % while *Nitrosomonadaceae*, representing AOB, accounted for 16.8 %, slightly outnumbering *Nitrospiraceae*, representing ComB, at 14.4 % (Figure 9.c). When including *amoA* sequencing results, a deeper distinction on genera level can be achieved as shown in Figure8 .

5.3.2 Ammonia oxidizer community analysis

The ammonia-oxidizing community was examined using *amoA* gene amplicon sequencing. The examination of AOA diversity (Figure 10) in the soil samples unveiled notable patterns across various taxonomic groups. All AOA found belonged to two distinct families, the *Nitrosopumilaceae* and the *Nitrososphaeraceae*. The *Nitrosopumilaceae* family contained a single representative from the genus *Nitrosarchaeum-NP-Gamma* and was exclusively detected in samples A and C, exhibiting minimal representation ranging from 0.06% to 0.11%. The *Nitrososphaeraceae* family constituted the majority of the AOA community and comprised the predominant genera. *TA-21 NS Delta* represents a significant proportion of the AOA community across all samples of around 65-74%. Additionally, *Nitrosocosmicus NS Beta* (2-12%) and *Nitrosocosmicus NS Epsilon* (7-14%) exhibited notable abundance, albeit not uniformly across all soil samples. Furthermore, a notable presence (7-16%) of unclassified taxa within the *Nitrososphaeraceae* family was noted, suggesting potential novel diversity within this group (Figure 10.b). In total 21 ASVs ($\geq$ 2%) were found to represent 70.8 % - 77.4 % of the AOA community (Figure 10.a)

Comammox clade B (ComB) *Nitrospira* was identified under the phylum Nitrospirota, class Nitrospiria, order Nitrospirales, and family Nitrospiraceae. Within this classification, all ComB

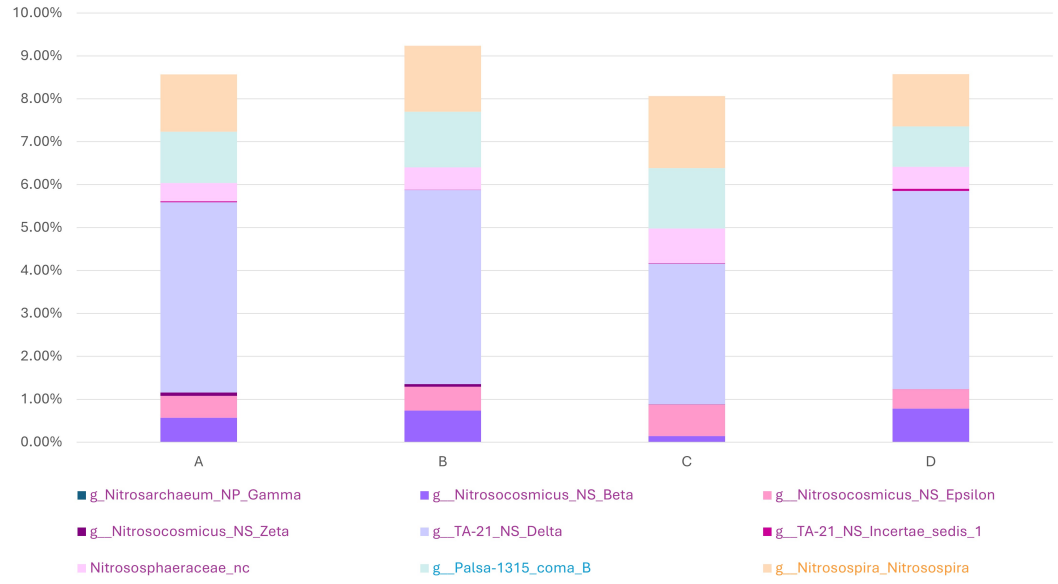

Figure 8: **Relative distribution of nitrifier genera within the entire microbial community:** Purple represents AOA, turquoise denotes ComB, and orange indicates AOB.

belonged to the genus Palsa-1315 (Figure 8). Comammox clade A was also detected, but in such low abundances, they are not included in the data analysis.
ASV distribution analysis showed 17 ASVs (each representing $\geq$ 2 % of the ComB community) making up 91.8 % - 99.2 % of the ComB community (Figure11)

The soil's AOB community was solely represented by the genus *Nitrosospira*, belonging to the family of *Nitrosomonadaceae*, the order of Burkholderiales, the class of Gammaproteobacteria inside the phylum of Proteobacteria. In AOB, 23 ASVs were found to exhibit $\geq$ 2% in at least one soil replicate (Figure 12). In total, these AOBs made up 86.9 % - 91.6 % of the whole AOB community.

5.3.3 Microbial diversity

The diversity of microbial communities was assessed across four plots (A, B, C, D) for three functional groups: ComB, AOA, and AOB as shown in Table11. Diversity metrics, including species richness, evenness, and Shannon diversity index, were calculated to evaluate the structure and distribution of ASVs within each group and across the study area. Richness in the ComB group varied across the plots, with Plot B exhibiting the highest richness (21 ASVs) and Plot C the lowest (15 ASVs). The overall richness for the ComB group across all plots was 23 ASVs. Evenness, which measures the distribution of ASVs within each plot, was highest in Plot C

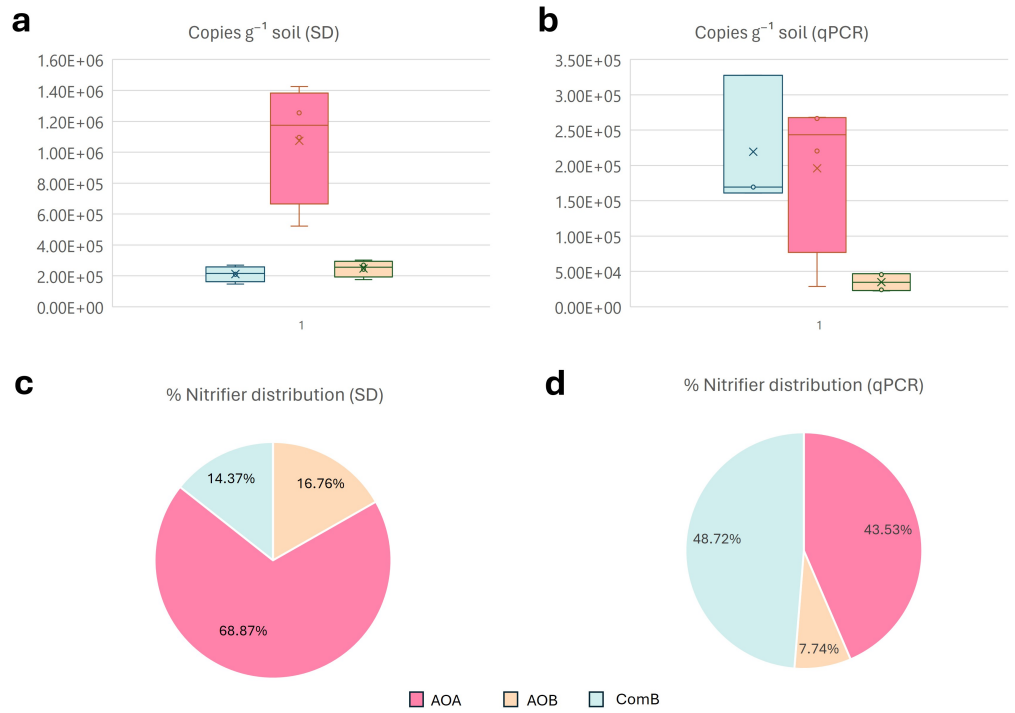

Figure 9: **Comparison between qPCR and quantification using sequence data (SD): (a,b)** depicts the absolute abundance of the different nitrifier clades (AOA, AOB, and ComB). **(b,d)** shows the relative abundance of each nitrifying clade

(0.85), indicating a more balanced distribution of ASVs. Plot B had the lowest evenness (0.76), suggesting a greater dominance of certain ASVs. The overall evenness for the ComB group was 0.78. The Shannon diversity index, which integrates both richness and evenness, was calculated as 2.46 for the entire ComB group, reflecting moderate diversity within this functional group.
The AOA group exhibited the highest ASV richness among the three groups, with richness values ranging from 79 ASVs in Plot C to 101 ASVs in Plot D. The overall richness for the AOA group was 123 ASVs, indicating a highly diverse community. Evenness across the plots was relatively consistent, with the highest evenness observed in Plot D (0.82) and the lowest in Plot C (0.76). The overall evenness for the AOA group was 0.78. The Shannon diversity index for AOA was 3.74, the highest among the three groups, suggesting that the AOA group not only has a high number of ASVs but also a relatively even distribution, contributing to its high overall diversity.
Species richness within the AOB group was more consistent across the plots compared to the other groups, with values ranging from 41 ASVs in Plot C to 47 ASVs in Plot B. The overall richness for AOB was 47 ASVs. Evenness was notably high in Plot C (0.87), indicating a very even distribution of ASVs. Plot D exhibited the lowest evenness (0.77). The overall evenness for the AOB group was 0.82, the highest among the three groups, reflecting a well-balanced

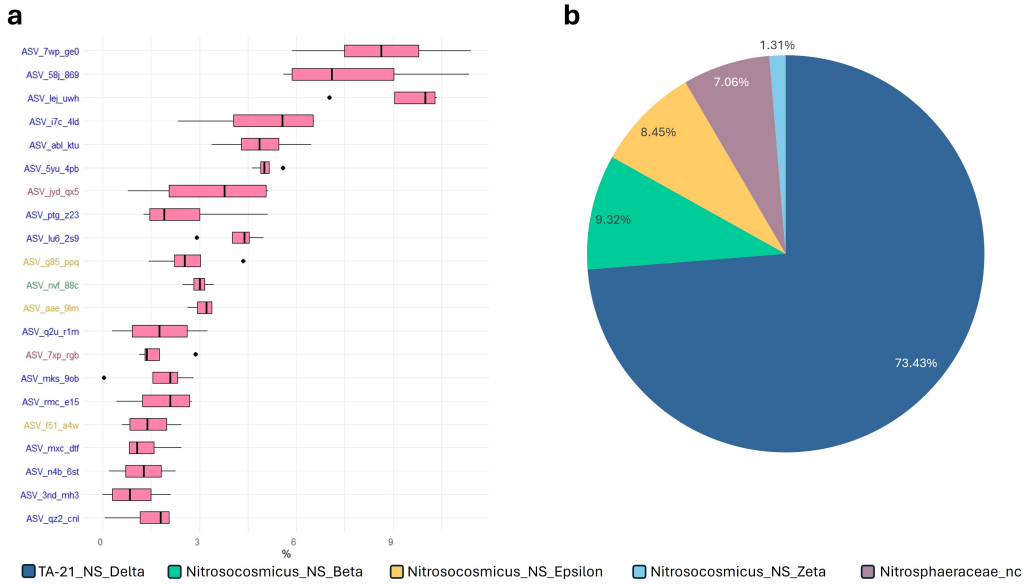

Figure 10: **AOA distribution:(a)** depicts the ASV distribution of the most abundant ASVs with each ASV making up $\geq$ 2% of the AOA community in at least one soil replicate.. ASV colors indicate their affiliation to a specific genera, **(b)** shows the overall diversity of the AOA community in %.

community structure. The Shannon diversity index for AOB was 3.15, indicating substantial diversity, though slightly lower than that observed in the AOA group.

Table 11: Microbial diversity across all soil replicates in ComB, AOA and AOB.

	ComB			AOA			AOB		
sampling site	richness	eveness	shannon	richness	eveness	shannon	richness	eveness	shannon
A	19	0.77	2.27	95	0.81	3.69	42	0.80	3.00
B	21	0.76	2.31	91	0.78	3.53	47	0.79	3.05
C	15	0.85	2.31	79	0.76	3.31	41	0.87	3.23
D	18	0.79	2.28	101	0.82	3.79	45	0.77	2.91
overall	23	0.78	2.46	123	0.78	3.74	47	0.82	3.15

5.3.4 Abundance

Each clade was quantified using qPCR, as described in the materials and methods section above. On average, $1.8x10^7 \pm 5.1x10^6$ 16S rRNA copies/g^{-1}DW soil were detected. The abundance of AOA *amoA* was measured at $1.9x10^5 \pm 1.3x10^5$ copies/g^{-1}DW soil, while AOB *amoA* and ComB accounted for $3.5x10^4 \pm 1.3x10^4$ and $2.2x10^5 \pm 9.3x10^4$ copies/g^{-1}DW soil, respectively (Figure 9.b).

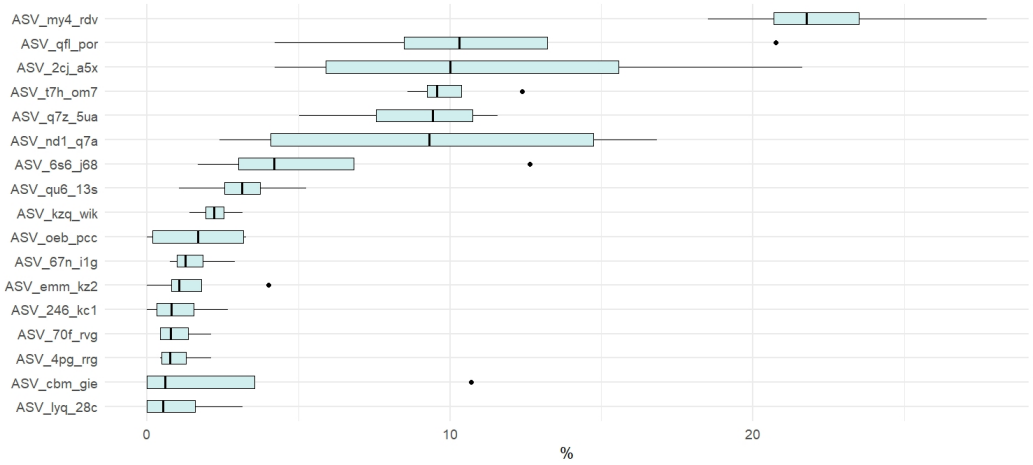

Figure 11: **ComB ASV distribution:** depicts the ASV distribution of the most abundant ASVs with each ASV making up $\geq$ 2% of the ComB community in at least one soil replicate.

When compared to the 16S rRNA, the proportion of each clade in the whole community, measured using qPCR, showed a distribution of 1.1 % for AOA, 0.5 % for AOB, and 1.3 % for ComB, diverging significantly from the percentages obtained from 16S rRNA gene amplicons sequencing (Figure 9.d)

Furthermore, the sequencing data was correlated with the 16S rRNA qPCR results to determine the absolute abundance for each clade (=sequence data = SD). AOA showed a final abundance of $1.1\text{x}10^6 \pm 3.9\text{x}10^5$, while for AOB and ComB, the absolute abundances were $2.5\text{x}10^5 \pm 5.4\text{x}10^4$ and $2.1\text{x}10^5 \pm 5\text{x}10^4$ copies of g^{-1} DW soil, respectively (Figure 9.a). Except for ComB, the values differed greatly from those obtained from the sequence data.

5.3.5 Transcription of *amoA* mRNA indicating activity

To assess the activity of ammonia-oxidizing microorganisms' expression of the *amoA* gene was quantified, using reverse transcription quantitative PCR (RT-qPCR). By targeting *amoA* mRNA, we aimed to measure the transcriptional activity of ammonia-oxidizing archaea (AOA) and bacteria (AOB), thereby providing insights into their functional roles in the studied environments. No detectable transcription was found for ComB and AOA. AOB showed an *amoA* copy number of 1.89 per µl, while 16S rRNA activity showed a 16S copy number of 193840.4 per µl. Active members of the AOB community therefore only made up a fraction of the whole microbial community as the *amoA* copy numbers resemble only 0.001 % of the 16S rRNA activity.

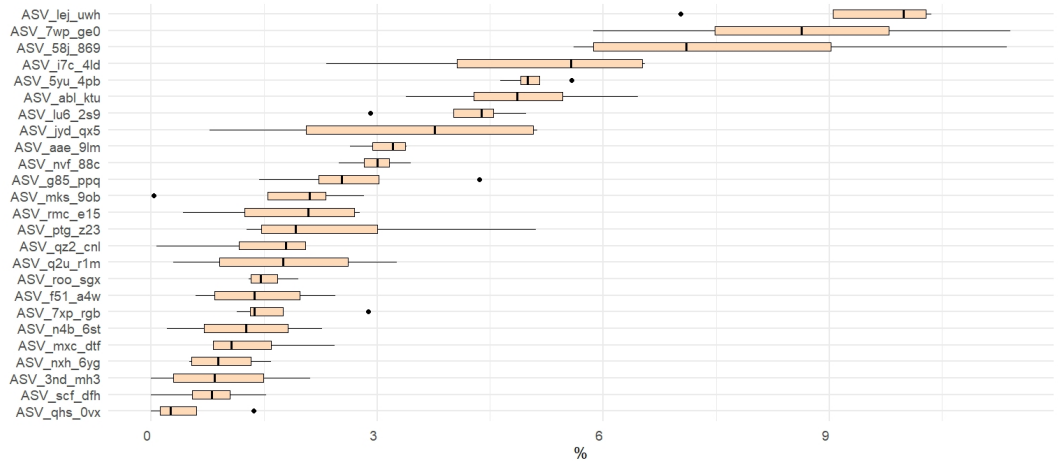

Figure 12: **AOB ASV distribution:** depicts the ASV distribution of the most abundant ASVs with each ASV making up $\geq$ 2% of the AOB community in at least one soil replicate..

6 Discussion

In this study, we focused on generating data on the efficiency of various BNIs in a specific soil type, with a particular emphasis on understanding the factors influencing their performance. Our results were compared to the findings from Rojas et al. (2023), who investigated BNI efficiency across two additional soil types. By contextualizing our data with their broader analysis, we aimed to gain deeper insights into how soil-specific parameters affect BNI efficiency and the activity of ammonia-oxidizing microorganisms (AOA and AOB). This comparative approach allows us to better understand the potential variability in BNI performance across different environmental contexts.

6.1 Differences in BNI efficiencies

Limonene exhibited the highest inhibitory potential in the Linz soil, followed by MHPA, whereas MHPP demonstrated the lowest efficiency. Across all three soils tested, MHPP consistently showed the lowest efficiency, as illustrated in Figure 5. Despite Limonene showing low EC50 values in Linz and Marchfeld, its efficiency was significantly lower in Wieselburg soil than MHPA, suggesting specific soil parameters may strongly influence the inhibitory efficiency of limonene.

Understanding the impact of soil conditions on the nitrification process and its effect on ammonia-oxidizing communities is crucial. The results from the correlation analysis between soil parameters and the EC50 values of specific compounds (MHPP, Limonene, MHPA), indicate distinct relationships that can inform our understanding of compound-soil interactions and the mode of

action for each compound.

The inverse relationship observed between total copper concentration and the EC50 values of MHPP and limonene implies that higher copper levels correspond to lower EC50 values, thus suggesting increased inhibitor efficiency. Many inhibitory compounds achieve their inhibitory potential by acting as copper chelators. By forming stable complexes between the inhibitor and the copper ions of the soil, the copper is no longer available for biological processes like nitrification. As the AMO enzyme is thought to have a Cu+ at its active site, depletion of available Cu+ would interfere with the production of the AMO enzyme, subsequently inhibiting the nitrification process. However, a copper-chelating mechanism for MHPP and limonene seems unlikely, as higher copper concentrations would suggest that a greater amount of the inhibitory substance is needed for significant nitrification inhibition Cu+ can also influence other soil characteristics, therefore having synergetic effects, which can affect nitrification. In general, Cu+ can affect the microbial community by suppressing or promoting specific groups of nitrifiers [118, 119]. Matse et al. (2023) propose that elevated Cu+ levels can exert a toxic impact on ammonia-oxidizing organisms, with a notably greater effect observed on ammonia-oxidizing bacteria (AOB) compared to ammonia-oxidizing archaea (AOA). This discrepancy in sensitivity could be attributed to variances in the composition of bacterial and archaeal cell walls, potentially rendering AOA more resistant than AOB to copper-induced toxicity. In this context, copper-chelating inhibitors may specifically target nitrifying populations susceptible to fluctuations in copper ion concentrations and might be targeting AOA more than AOB.
While copper ions (Cu+) can influence soil pH by releasing protons during their adsorption onto soil particles, our findings do not indicate this as a significant factor in our soils, as the correlation between pH and Cu+ content is below 0,1.

6.1.1 pH and organic C content

While pH does not seem to influence the efficiency of MHPP and Limonene, we found a high correlation between pH and MHPA (R^2 = 0,93). Since both MHPA and MHPP contain a phenolic group, the protonation of this group might significantly impact their efficiency. However, they differ in their chemical structures: MHPA has an , unsaturated ester moiety, whereas MHPP has a saturated ester moiety. These structural differences could influence pH-dependent changes in the compounds, as saturated ester moieties are less reactive than α/β-unsaturated ester moieties. This could explain pH-dependent efficiencies in MHPA, while MHPP seems nonaffected. On the other hand, recent studies suggest that not pH but rather other soil characteristics such as organic matter content could be a driving factor [120, 96]. In this study, we observe an intercorrelation between soil pH and total carbon content (R^2 = 0,98). High organic matter content is thought to increase the sorption of organic compounds to the soil and could therefore decrease the efficiency of NIs. Mardsen et al. (2016) also suggest that different compounds exhibit varying susceptibility to this sorption process. This might explain the diverse correlation patterns observed in total carbon content among the three tested nitrification inhibitors. Conversely, the inverse relationship between soil pH and MHPA EC50 values implies that acidic conditions may enhance the efficiency of MHPA, possibly by facilitating its bioavailability or chemical transformation. Additionally, the positive association between soil sodium content and MHPA EC50

values underscores the potential influence of soil salinity on compound efficiency.
Nevertheless, as only 3 soils were tested, the results of this study can only be seen as preliminary tendencies as more studies with different soil types would be needed to achieve well-grounded results. Additionally, due to the strong intercorrelation between pH and organic carbon content, it is not possible to determine which factor is the decisive one.

6.2 AOA activity vs. abundance

According to the RT qPCR data, *amoA* transcription from AOA was undetectable in fresh soil, consistent with the outcomes of the initial experiment, which revealed no notable contrast between the total inhibitor phenylacetylene and the bacterial-specific inhibitor octyne (Δ NO_3^- = 1.2 µM g^{-1} soil DW). Interestingly, the subsequent experiment exhibited distinctions among the phenylacetylene and octyne control groups, with the octyne treatment accumulating 7.3 µM g^{-1} soil DW more NO_3^- than the phenylacetylene treatment. Experiment 1 and Experiment 2 were carried out with a 2-week interval, during which the soil utilized for the experiment was stored at 4°C. Tourna et. al (2008) suggest that temperature differences can alter the AOA community [121]. Anyway, the increased activity of AOA observed is likely not directly attributable to the decreased temperature, as AOA generally has higher optimal growth temperatures compared to AOB [122]. Instead, the heightened AOA activity is probably due to changes in heterotrophic microbial activity during the storage period. Alterations in the microbial community or a reduction in heterotrophic activity could have indirectly influenced the conditions, such as decreasing ammonia availability, thereby promoting the activity of AOA, which are specialised on low NO_3^- and resulting in increased NO_3^- production.
However, the overall activity of AOA remained low, which strongly contrasts with the abundant numbers discovered. The total contribution of AOA to soil nitrification, especially in arable soils is still an open question and seems to differ greatly, depending on the soil [123, 5].
It is still unclear how the tested BNIs differentiate in their effect on bacteria and archaea. In general, AOA may generally be less vulnerable than its bacterial counterpart to inhibitory substances, possibly due to variances in archaeal cell walls and membranes [123]. Future studies could benefit from examining changes in microbial composition following incubation with BNIs, to better evaluate their effects on various microbial groups.

6.3 qPCR vs. quantification via 16S rRNA gene sequencing

Addressing the discrepancy in the quantification of nitrifying clades using amoA gene-targeted qPCR versus sequencing methods, we observe a significant difference. A detailed comparison between qPCR and sequencing data revealed notable discrepancies, particularly for AOA, where qPCR measurements accounted for only 18.3 % of the abundance estimated from sequencing data. Similarly, AOB abundance measured by qPCR comprised only 14.1 % of the sequencing data estimate. Conversely, ComB abundances displayed similar numbers in both qPCR and sequencing methods, suggesting a potential methodological bias or inherent differences in detection efficiency between the two approaches. Given that the sequence data is derived from 16S rRNA gene sequencing, which requires careful consideration due to its limitations, it is

important to note that 16S rRNA gene phylogenies cannot distinguish whether a *Nitrospira* bacteria is a comammox or a NOB [36]. However, the similarity to the qPCR data supports a high level of confidence in the estimated numbers. Compared to present literature ([124, 27]) the sequence data reflects commonly observed patterns with AOA being the most abundant clade while ComB and AOB are less abundant. This would indicate a strong bias in the AOA qPCR data. This bias could be accounted for by the broad genus distribution as seen in Figure 10. Especially the percentage of non-classified *Nitrososphaeraceae* (7.1 %) indicates phylogenetic novelty with possible variations in their *amoA* sequence that might not be targeted by the primers used, while on the family level, they can still be detected through 16S rRNA gene sequencing, which could account for the higher numbers observed. In general, AOA exhibit high genetic diversity, complicating the design of primers that are universally specific to all AOA clades, possibly resulting in non-specific amplification or underestimation of AOA abundance by not targeting all AOA genera. Additionally to AOA, AOB numbers also differ greatly between both quantification methods as the sequence data shows values almost 7 times higher than the qPCR data indicating a possible strong underestimation of AOBs through qPCR. Another explanation for the abundance discrepancy is primer biases caused by 16S rRNA gene sequencing. Due to primer preferences for specific sequences/organisms, there might be some overrepresentation or underrepresentation of particular groups in the resulting data.
In general, the AOA and AOB numbers in our study were lower than previously reported. Recent studies have noted varying *amoA* gene copy numbers per g of dry soil for AOA and AOB in agricultural soils, with AOA numbers ranging from 10^6 to 10^8 and AOB numbers from 10^4 to 10^7, while our studies showed values for AOA between 10^5 and 10^6 and AOB *amoA* copy numbers between 10^4 and 10^5 [125, 126, 127].
The discrepancies observed between *amoA*-specific qPCR and sequencing methods underscore the complexities involved in microbial quantification. While *amoA*-specific qPCR provides high sensitivity and specificity for target genes, it may be influenced by primer biases, lack of primer specificity, and differential amplification efficiencies. 16S rRNA sequencing, on the other hand, offers a broader snapshot of microbial diversity but may suffer from biases in library preparation, and sequencing depth. These methodological differences highlight the need for careful interpretation of microbial abundance data and suggest that combining multiple approaches may provide a more comprehensive understanding of microbial community structure.

6.4 Microbial Community Diversity Across Functional Groups

The diversity analysis of the microbial communities across the different plots and functional groups (ComB, AOA, AOB) revealed distinct patterns of richness, evenness, and overall diversity that provide insights into the ecological roles and adaptability of these groups within the studied environment.
The AOA group exhibited the highest species richness across all plots, indicating a broad diversity of taxa within this group which aligns with findings from other studies that have reported similar results[32]. This high richness suggests that AOA may occupy a wide range of ecological niches, potentially driven by the variability in environmental conditions across the plots. In contrast, the AOB group, while showing lower richness overall, may represent a more specialized

community, perhaps adapted to specific conditions or resources available in the environment. Evenness was highest in the AOB group, particularly in Plot C, suggesting that the taxa within this group are more evenly distributed, which may reflect a balanced competition among species. The lower evenness observed in the AOA group, despite its high richness, may indicate the presence of dominant species that outcompete others, potentially due to specific adaptations or competitive advantages. The ComB group showed moderate evenness across the plots, with Plot C standing out as having the most balanced distribution. This pattern could reflect varying degrees of niche specialization and competition within the microbial communities, with implications for the stability and resilience of these ecosystems.

The Shannon diversity index, which integrates both richness and evenness, was highest for the AOA group, underscoring the extensive diversity of taxa within this functional group. This high diversity may confer resilience to environmental changes, as a greater variety of species increases the likelihood that some will thrive under shifting conditions. The AOB group had a slightly lower Shannon index, demonstrating a higher evenness but lower diversity, which may contribute to its functional importance within specific ecological contexts, such as nitrification processes. The ComB group, while exhibiting the lowest Shannon diversity, maintains a significant level of diversity, which could reflect a stable and functionally diverse community capable of sustaining key microbial processes.

The observed patterns of diversity are consistent with previous studies that have reported high richness and diversity in AOA communities, particularly in heterogeneous environments where multiple niches are available[32]. Similarly, the relatively high evenness in AOB communities aligns with findings that suggest these bacteria thrive in more stable or nutrient-rich environments where competition is less intense [21, 14].

The diversity metrics observed in this study suggest that the AOA group may play a critical role in maintaining ecosystem functioning due to its high richness and diversity in changing environmental conditions, which likely supports a wide range of metabolic activities. The dominance of specific taxa within the AOB group highlights their significant influence on the nitrification process in this study, as species dominance generally occurs when resources are efficiently utilized. This competitive advantage allows them to proliferate, thereby playing a crucial role in the nitrification process.

6.5 DMSO as a nitrification inhibitor

Dimethyl sulfoxide (DMSO) is a sulfur-containing organic solvent which can have a complex impact on nitrification. According to G.W. McCarty (1999) and Hauck et al. (1980), S-containing compounds like DMSO can inhibit nitrification by interacting with the copper active site of the AMO. However, its effects can be dosage-dependent, as indicated by recent data suggesting varying toxicity levels of DMSO [128, 129]. Contrastingly, some studies have reported no significant effect of DMSO on nitrification [130, 96]. In our observations, there was a difference between the MQ and DMSO controls in terms of NO_3^- accumulation and potential nitrification rates, pointing to a possible inhibitory effect of DMSO although not significant (p = 0,59). Given DMSO's chemical structure, which includes an internal C=S group, it is plausible that this component contributes to the reduced NO_3^- accumulation observed. Until now there is

no designated explanation for the differing effect of DMSO on nitrification potential. However, it can be suggested, that differences in soil characteristics might be the missing link.

6.6 Outlook on N-trends in the future

As food production continues to rise, the production of reactive nitrogen will also increase. Consequently, this will lead to greater deposition of nitrogen compounds in soil and aquatic systems, as well as higher emissions of N_2O.[15]. Additionally, biofuels are getting increasingly more attention. Therefore, it becomes imperative to scrutinize future trends in this domain, particularly regarding their impact on the global nitrogen cycle. Similar to food production, nitrogen use efficiency (NUE) in biofuel cultivation remains notably low, with only approximately 30% of nitrogen being utilized by plants [131]. Recent trends indicate a significant expansion in agricultural land allocated for biofuel production, potentially leading to a doubling of such areas. While this expansion aims to mitigate CO_2 emissions, it raises concerns about nitrogen pollution, notably through increased production of N_2O and tropospheric ozone (O_3) [132]. Another concern regarding nitrogen pollution pertains to the unequal distribution of food production, as imports and exports play a substantial role in global trade. Consequently, certain countries produce an excess of food beyond their domestic needs. A significant portion of this surplus food, along with its nitrogen content, is exported, while the nitrogen lost during the food production process remains within the producing country. This retention contributes to heightened levels of groundwater pollution, ambient ammonia, particle emissions, and nitrogen deposition [133].

Since Johann Rockström introduced "planetary boundaries" in 2009, the nitrogen cycle has been categorized as a critical zone of concern due to its "high risk" status [134, 135, 136]. This designation underscores the urgent need for sustainable strategies to address imbalances in the N-cycle. Biological nitrification inhibitors represent a promising approach to mitigate issues such as NO_3^- pollution and N_2O emissions. Despite their potential, there remains a significant gap in understanding the factors that influence BNI efficiency, optimal application methods, and production management. Advancing research in these areas is essential to fully leverage BNIs for environmental protection and sustainability.

References

[1] Lisa Y Stein and Martin G Klotz. "The nitrogen cycle". In: *Current Biology* 26.3 (2016), R94–R98.

[2] Will Hollingsworth. *Our Changing Planet: An Introduction to Earth System Science and Global Environmental Change*. 1998.

[3] Eberhard Bock and Michael Wagner. "Oxidation of inorganic nitrogen compounds as an energy source". In: *The prokaryotes* 2 (2006), pp. 457–495.

[4] James Ivor Prosser. "Autotrophic nitrification in bacteria". In: *Advances in microbial physiology* 30 (1990), pp. 125–181.

[5] S Leininger et al. "Archaea predominate among ammonia-oxidizing prokaryotes in soils". In: *Nature* 442.7104 (2006), pp. 806–809.

[6] Jonathan D Caranto and Kyle M Lancaster. "Nitric oxide is an obligate bacterial nitrification intermediate produced by hydroxylamine oxidoreductase". In: *Proceedings of the National Academy of Sciences* 114.31 (2017), pp. 8217–8222.

[7] Holger Daims et al. "Complete nitrification by Nitrospira bacteria". In: *Nature* 528.7583 (2015), pp. 504–509.

[8] Maartje AHJ Van Kessel et al. "Complete nitrification by a single microorganism". In: *Nature* 528.7583 (2015), pp. 555–559.

[9] J Gijs Kuenen. "Anammox bacteria: from discovery to application". In: *Nature Reviews Microbiology* 6.4 (2008), pp. 320–326.

[10] Pierfrancesco Nardi et al. "Biological nitrification inhibition in the rhizosphere: determining interactions and impact on microbially mediated processes and potential applications". In: *FEMS Microbiology Reviews* 44.6 (2020), pp. 874–908.

[11] Jinbo Zhang et al. "The substrate is an important factor in controlling the significance of heterotrophic nitrification in acidic forest soils". In: *Soil Biology and Biochemistry* 76 (2014), pp. 143–148.

[12] James WB Moir et al. "The purification of ammonia monooxygenase from Paracoccus denitrficans". In: *FEBS letters* 387.1 (1996), pp. 71–74.

[13] Roger Knowles. "Denitrification". In: *Microbiological reviews* 46.1 (1982), pp. 43–70.

[14] Bin Ji et al. "Aerobic denitrification: a review of important advances of the last 30 years". In: *Biotechnology and bioprocess engineering* 20 (2015), pp. 643–651.

[15] James N Galloway et al. "Nitrogen cycles: past, present, and future". In: *Biogeochemistry* 70 (2004), pp. 153–226.

[16] Sophie Wertz et al. "Maintenance of soil functioning following erosion of microbial diversity". In: *Environmental microbiology* 8.12 (2006), pp. 2162–2169.

[17] Sophie Wertz et al. "Decline of soil microbial diversity does not influence the resistance and resilience of key soil microbial functional groups following a model disturbance". In: *Environmental microbiology* 9.9 (2007), pp. 2211–2219.

[18] James I Prosser. "Soil nitrifiers and nitrification". In: *Nitrification* (2011), pp. 347–383.

[19] Noah J Langenfeld et al. "Optimizing nitrogen fixation and recycling for food production in regenerative life support systems". In: *Frontiers in Astronomy and Space Sciences* 8 (2021), p. 699688.

[20] Ji-Zheng He, Hang-Wei Hu, and Li-Mei Zhang. "Current insights into the autotrophic thaumarchaeal ammonia oxidation in acidic soils". In: *Soil Biology and Biochemistry* 55 (2012), pp. 146–154.

[21] Hong J Di et al. "Ammonia-oxidizing bacteria and archaea grow under contrasting soil nitrogen conditions". In: *FEMS microbiology ecology* 72.3 (2010), pp. 386–394.

[22] K Dimitri Kits et al. "Kinetic analysis of a complete nitrifier reveals an oligotrophic lifestyle". In: *Nature* 549.7671 (2017), pp. 269–272.

[23] Edwin L Schmidt. "Nitrification in soil". In: *Nitrogen in agricultural soils* 22 (1982), pp. 253–288.

[24] KL Sahrawat. "Factors affecting nitrification in soils". In: *Communications in Soil Science and Plant Analysis* 39.9-10 (2008), pp. 1436–1446.

[25] DT Strong, PWG Sale, and KR Helyar. "The influence of the soil matrix on nitrogen mineralisation and nitrification. IV. Texture". In: *Soil Research* 37.2 (1999), pp. 329–344.

[26] George A Kowalchuk and John R Stephen. "Ammonia-oxidizing bacteria: a model for molecular microbial ecology". In: *Annual Reviews in Microbiology* 55.1 (2001), pp. 485–529.

[27] Christa Schleper and Graeme W Nicol. "Ammonia-oxidising archaea–physiology, ecology and evolution". In: *Advances in microbial physiology* 57 (2010), pp. 1–41.

[28] Roland Hatzenpichler. "Diversity, physiology, and niche differentiation of ammonia-oxidizing archaea". In: *Applied and environmental microbiology* 78.21 (2012), pp. 7501–7510.

[29] Torsten Ochsenreiter et al. "Diversity and abundance of Crenarchaeota in terrestrial habitats studied by 16S RNA surveys and real time PCR". In: *Environmental Microbiology* 5.9 (2003), pp. 787–797.

[30] Roland Hatzenpichler et al. "A moderately thermophilic ammonia-oxidizing crenarchaeote from a hot spring". In: *Proceedings of the National Academy of Sciences* 105.6 (2008), pp. 2134–2139.

[31] José R De la Torre et al. "Cultivation of a thermophilic ammonia oxidizing archaeon synthesizing crenarchaeol". In: *Environmental microbiology* 10.3 (2008), pp. 810–818.

[32] Antoni Fernandez-Guerra and Emilio O Casamayor. "Habitat-associated phylogenetic community patterns of microbial ammonia oxidizers". In: (2012).

[33] Cécile Gubry-Rangin, Graeme W Nicol, and James I Prosser. "Archaea rather than bacteria control nitrification in two agricultural acidic soils". In: *FEMS microbiology ecology* 74.3 (2010), pp. 566–574.

[34] Christopher B Walker et al. “Nitrosopumilus maritimus genome reveals unique mechanisms for nitrification and autotrophy in globally distributed marine crenarchaea”. In: *Proceedings of the National Academy of Sciences* 107.19 (2010), pp. 8818–8823.

[35] Engràcia Costa, Julio Pérez, and Jan-Ulrich Kreft. “Why is metabolic labour divided in nitrification?” In: *Trends in microbiology* 14.5 (2006), pp. 213–219.

[36] Petra Pjevac et al. “AmoA-targeted polymerase chain reaction primers for the specific detection and quantification of comammox Nitrospira in the environment”. In: *Frontiers in microbiology* 8 (2017), p. 1508.

[37] Xiuzhen Shi et al. “Niche separation of comammox Nitrospira and canonical ammonia oxidizers in an acidic subtropical forest soil under long-term nitrogen deposition”. In: *Soil Biology and Biochemistry* 126 (2018), pp. 114–122.

[38] Zhihui Wang et al. “Comammox Nitrospira clade B contributes to nitrification in soil”. In: *Soil Biology and Biochemistry* 135 (2019), pp. 392–395.

[39] Holger Daims, Sebastian Lücker, and Michael Wagner. “A new perspective on microbes formerly known as nitrite-oxidizing bacteria”. In: *Trends in microbiology* 24.9 (2016), pp. 699–712.

[40] Andreas Schramm et al. “Microscale distribution of populations and activities of Nitrosospira and Nitrospira spp. along a macroscale gradient in a nitrifying bioreactor: quantification by in situ hybridization and the use of microsensors”. In: *Applied and environmental microbiology* 65.8 (1999), pp. 3690–3696.

[41] Silke Ehrich et al. “A new obligately chemolithoautotrophic, nitrite-oxidizing bacterium, Nitrospira moscoviensis sp. nov. and its phylogenetic relationship”. In: *Archives of microbiology* 164 (1995), pp. 16–23.

[42] Sebastian Lücker et al. “A Nitrospira metagenome illuminates the physiology and evolution of globally important nitrite-oxidizing bacteria”. In: *Proceedings of the National Academy of Sciences* 107.30 (2010), pp. 13479–13484.

[43] David S LeBauer and Kathleen K Treseder. “Nitrogen limitation of net primary productivity in terrestrial ecosystems is globally distributed”. In: *Ecology* 89.2 (2008), pp. 371–379.

[44] Jan Willem Erisman et al. “How a century of ammonia synthesis changed the world”. In: *Nature geoscience* 1.10 (2008), pp. 636–639.

[45] David Fowler et al. “The global nitrogen cycle in the twenty-first century”. In: *Philosophical Transactions of the Royal Society B: Biological Sciences* 368.1621 (2013), p. 20130164.

[46] Guntur Venkata Subbarao et al. “Suppression of soil nitrification by plants”. In: *Plant Science* 233 (2015), pp. 155–164.

[47] Kenneth G Cassman, Achim Dobermann, and Daniel T Walters. “Agroecosystems, nitrogen-use efficiency, and nitrogen management”. In: *AMBIO: A Journal of the Human Environment* 31.2 (2002), pp. 132–140.

[48] Martin Kuecke. “Anbauverfahren mit N-Injektion (CULTAN): Ergebnisse, Perspektiven, Erfahrungen”. In: (2003).

[49] RH McKenzie et al. “Controlled-release urea for winter wheat in southern Alberta”. In: *Canadian Journal of Soil Science* 87.1 (2007), pp. 85–91.

[50] Xiaolin Fan et al. “Fertilization with a new type of coated urea: Evaluation for nitrogen efficiency and yield in winter wheat”. In: *Journal of plant nutrition* 27.5 (2004), pp. 853–865.

[51] William H Schlesinger. “On the fate of anthropogenic nitrogen”. In: *Proceedings of the National Academy of Sciences* 106.1 (2009), pp. 203–208.

[52] Laura E Lehtovirta-Morley. “Ammonia oxidation: ecology, physiology, biochemistry and why they must all come together”. In: *FEMS microbiology letters* 365.9 (2018), fny058.

[53] Mark A Sutton et al. “Towards a climate-dependent paradigm of ammonia emission and deposition”. In: *Philosophical Transactions of the Royal Society B: Biological Sciences* 368.1621 (2013), p. 20130166.

[54] SN Singh and Amitosh Verma. “The potential of nitrification inhibitors to manage the pollution effect of nitrogen fertilizers in agricultural and other soils: a review”. In: *Environmental Practice* 9.4 (2007), p. 266.

[55] JM Bremner and Anda M Blackmer. “Nitrous oxide: emission from soils during nitrification of fertilizer nitrogen”. In: *Science* 199.4326 (1978), pp. 295–296.

[56] Carolien Kroeze. “Nitrous oxide and global warming”. In: *Science of the total environment* 143.2-3 (1994), pp. 193–209.

[57] Gesche Braker and Ralf Conrad. “Diversity, structure, and size of N2O-producing microbial communities in soils—what matters for their functioning?” In: *Advances in applied microbiology* 75 (2011), pp. 33–70.

[58] AR Ravishankara, John S Daniel, and Robert W Portmann. “Nitrous oxide (N2O): the dominant ozone-depleting substance emitted in the 21st century”. In: *science* 326.5949 (2009), pp. 123–125.

[59] G Philip Robertson. “Fluxes of nitrous oxide and other nitrogen trace gases from intensively managed landscapes: A global perspective”. In: *Agricultural ecosystem effects on trace gases and global climate change* 55 (1993), pp. 95–108.

[60] John M Bremner. “Sources of nitrous oxide in soils”. In: *Nutrient cycling in Agroecosystems* 49 (1997), pp. 7–16.

[61] Susan Solomon. *Climate change 2007-the physical science basis: Working group I contribution to the fourth assessment report of the IPCC*. Vol. 4. Cambridge university press, 2007.

[62] Linda Hink, Graeme W Nicol, and James I Prosser. “Archaea produce lower yields of N2O than bacteria during aerobic ammonia oxidation in soil”. In: *Environmental microbiology* 19.12 (2017), pp. 4829–4837.

[63] James I Prosser et al. “Nitrous oxide production by ammonia oxidizers: physiological diversity, niche differentiation and potential mitigation strategies”. In: *Global Change Biology* 26.1 (2020), pp. 103–118.

[64] Francesco Musiani et al. “The model structure of the copper-dependent ammonia monooxygenase”. In: *JBIC Journal of Biological Inorganic Chemistry* 25 (2020), pp. 995–1007.

[65] Ronald F Follett and Jerry L Hatfield. “Nitrogen in the environment: sources, problems and management”. In: (2001).

[66] Logan H Hodgskiss et al. “Unexpected complexity of the ammonia monooxygenase in archaea”. In: *The ISME Journal* 17.4 (2023), pp. 588–599.

[67] Fabian Beeckman, Hans Motte, and Tom Beeckman. “Nitrification in agricultural soils: impact, actors and mitigation”. In: *Current opinion in Biotechnology* 50 (2018), pp. 166–173.

[68] GW McCarty. “Modes of action of nitrification inhibitors”. In: *Biology and Fertility of Soils* 29 (1999), pp. 1–9.

[69] Luis A Sayavedra-Soto and Daniel J Arp. “Ammonia-oxidizing bacteria: their biochemistry and molecular biology”. In: *Nitrification* (2011), pp. 9–37.

[70] David A Stahl and José R De La Torre. “Physiology and diversity of ammonia-oxidizing archaea”. In: *Annual review of microbiology* 66 (2012), pp. 83–101.

[71] Ronald D Jones and Richard Y Morita. “Methane oxidation by Nitrosococcus oceanus and Nitrosomonas europaea”. In: *Applied and Environmental Microbiology* 45.2 (1983), pp. 401–410.

[72] KF Bronson and AR Mosier. “Suppression of methane oxidation in aerobic soil by nitrogen fertilizers, nitrification inhibitors, and urease inhibitors”. In: *Biology and Fertility of Soils* 17 (1994), pp. 263–268.

[73] James Allan Zahn. *Bacterial physiology and enzymology of the membrane-associated methane monooxygenase and ammonia oxidation system from Methylococcus capsulatus Bath, 1992-1996*. Iowa State University, 1996.

[74] Jack A Lewis and Robert L Starkey. “Vegetable tannins, their decomposition and effects on decomposition of some organic compounds”. In: *Soil Science* 106.4 (1968), pp. 241–247.

[75] Noah Fierer et al. “Influence of balsam poplar tannin fractions on carbon and nitrogen dynamics in Alaskan taiga floodplain soils”. In: *Soil Biology and Biochemistry* 33.12-13 (2001), pp. 1827–1839.

[76] Yan Ma et al. “Relative efficacy and stability of biological and synthetic nitrification inhibitors in a highly nitrifying soil: Evidence of apparent nitrification inhibition by linoleic acid and linolenic acid”. In: *European Journal of Soil Science* 72.6 (2021), pp. 2356–2371.

[77] T Rosswall. “Microbiological regulation of the biogeochemical nitrogen cycle/Regulación microbiana del ciclo bıogeoquımico del nitrógeno”. In: *Plant and Soil* (1982), pp. 15–34.

[78] Kyle M Lancaster et al. “Alternative bioenergy: updates to and challenges in nitrification metalloenzymology”. In: *Joule* 2.3 (2018), pp. 421–441.

[79] Claudia Gilsanz et al. “Development of emission factors and efficiency of two nitrification inhibitors, DCD and DMPP”. In: *Agriculture, Ecosystems & Environment* 216 (2016), pp. 1–8.

[80] Jeffrey D Wolt. “A meta-evaluation of nitrapyrin agronomic and environmental effectiveness with emphasis on corn production in the Midwestern USA”. In: *Nutrient Cycling in Agroecosystems* 69 (2004), pp. 23–41.

[81] Reiner Ruser and Rudolf Schulz. “The effect of nitrification inhibitors on the nitrous oxide (N2O) release from agricultural soils—a review”. In: *Journal of Plant Nutrition and Soil Science* 178.2 (2015), pp. 171–188.

[82] Todd Vannelli and Alan B Hooper. “Oxidation of nitrapyrin to 6-chloropicolinic acid by the ammonia-oxidizing bacterium Nitrosomonas europaea”. In: *Applied and Environmental Microbiology* 58.7 (1992), pp. 2321–2325.

[83] Emily E Woodward et al. “Widespread use of the nitrification inhibitor nitrapyrin: Assessing benefits and costs to agriculture, ecosystems, and environmental health”. In: *Environmental science & technology* 55.3 (2021), pp. 1345–1353.

[84] Ashok K Patra et al. “Effects of management regime and plant species on the enzyme activity and genetic structure of N-fixing, denitrifying and nitrifying bacterial communities in grassland soils”. In: *Environmental Microbiology* 8.6 (2006), pp. 1005–1016.

[85] S Guo et al. “Effect of ammonium and nitrate nutrition on some physiological processes in higher plants-growth, photosynthesis, photorespiration, and water relations”. In: *Plant Biology* (2006), pp. 21–29.

[86] Dev T Britto and Herbert J Kronzucker. “Ecological significance and complexity of N-source preference in plants”. In: *Annals of botany* 112.6 (2013), pp. 957–963.

[87] Rahul Sadhukhan et al. “Biological nitrification inhibition for sustainable crop production”. In: *Plant perspectives to global climate changes*. Elsevier, 2022, pp. 135–150.

[88] Hossain AKM Zakir et al. “Detection, isolation and characterization of a root-exuded compound, methyl 3-(4-hydroxyphenyl) propionate, responsible for biological nitrification inhibition by sorghum (Sorghum bicolor)”. In: *New Phytologist* 180.2 (2008), pp. 442–451.

[89] GV Subbarao et al. “Evidence for biological nitrification inhibition in Brachiaria pastures”. In: *Proceedings of the National Academy of Sciences* 106.41 (2009), pp. 17302–17307.

[90] Li Sun et al. “Biological nitrification inhibition by rice root exudates and its relationship with nitrogen-use efficiency”. In: *New Phytologist* 212.3 (2016), pp. 646–656.

[91] Cathryn A O’Sullivan et al. “Identification of several wheat landraces with biological nitrification inhibition capacity”. In: *Plant and Soil* 404 (2016), pp. 61–74.

[92] GV Subbarao et al. “Can biological nitrification inhibition (BNI) genes from perennial Leymus racemosus (Triticeae) combat nitrification in wheat farming?” In: *Plant and Soil* 299.1-2 (2007), pp. 55–64.

[93] Maoxing Zhang et al. “BNI-release mechanisms in plant root systems: current status of understanding”. In: *Biology and Fertility of Soils* 58.3 (2022), pp. 225–233.

[94] GV Subbarao et al. “Biological nitrification inhibition—a novel strategy to regulate nitrification in agricultural systems”. In: *Advances in agronomy* 114 (2012), pp. 249–302.

[95] GV Subbarao et al. “NH 4+ triggers the synthesis and release of biological nitrification inhibition compounds in Brachiaria humidicola roots”. In: *Plant and Soil* 290 (2007), pp. 245–257.

[96] Paula A Rojas-Pinzon et al. “Inhibition profile of three biological nitrification inhibitors and their response to soil pH modification in two contrasting soils”. In: *FEMS Microbiology Ecology* (2024), fiae072.

[97] Yangyang Liu et al. “The nitrification inhibitor methyl 3-(4-hydroxyphenyl) propionate modulates root development by interfering with auxin signaling via the NO/ROS pathway”. In: *Plant Physiology* 171.3 (2016), pp. 1686–1703.

[98] Subramaniam Gopalakrishnan et al. “Nitrification inhibitors from the root tissues of Brachiaria humidicola, a tropical grass”. In: *Journal of agricultural and food chemistry* 55.4 (2007), pp. 1385–1388.

[99] R Sylvester-Bradley, D Mosquera, and JE Mendez. “Inhibition of nitrate accumulation in tropical grassland soils: effect of nitrogen fertilization and soil disturbance”. In: *Journal of Soil Science* 39.3 (1988), pp. 407–416.

[100] T Ishikawa et al. “Suppression of nitrification and nitrous oxide emission by the tropical grass Brachiaria humidicola”. In: *Roots: The Dynamic Interface between Plants and the Earth: The 6th Symposium of the International Society of Root Research, 11–15 November 2001, Nagoya, Japan*. Springer. 2003, pp. 413–419.

[101] BB Ward, KJ Courtney, and JH Langenheim. “Inhibition of Nitrosomonas europaea by monoterpenes from coastal redwood (Sequoia sempervirens) in whole-cell studies”. In: *Journal of Chemical Ecology* 23 (1997), pp. 2583–2598.

[102] Carleton S White. “Nitrification inhibition by monoterpenoids: theoretical mode of action based on molecular structures”. In: *Ecology* 69.5 (1988), pp. 1631–1633.

[103] Taru Lehtinen et al. “Long-term amendment of four different compost types on a loamy silt Cambisol: impact on soil organic matter, nutrients and yields”. In: *Archives of Agronomy and Soil Science* 63.5 (2017), pp. 663–673.

[104] M Ros et al. “Hydrolase activities, microbial biomass and bacterial community in a soil after long-term amendment with different composts”. In: *Soil Biology and Biochemistry* 38.12 (2006), pp. 3443–3452.

[105] M Ros et al. “Long-term effects of compost amendment of soil on functional and structural diversity and microbial activity”. In: *Soil use and management* 22.2 (2006), pp. 209–218.

[106] K Aichberger and J Söllinger. "Use of biocompost in agriculture–results of a long-term field trial". In: *Realising the ETAP in the management of waste from farms, edited by: Spiegel, H. and Zonno, V., Proceedings of the second AQUAGRIS workshop Vienna*. Vol. 19. 2009, pp. 6–8.

[107] Rebecca Hood-Nowotny et al. "Alternative methods for measuring inorganic, organic, and total dissolved nitrogen in soil". In: *Soil Science Society of America Journal* 74.3 (2010), pp. 1018–1027.

[108] Ellen Kandeler and H Gerber. "Short-term assay of soil urease activity using colorimetric determination of ammonium". In: *Biology and fertility of Soils* 6 (1988), pp. 68–72.

[109] Katrina M Miranda, Michael G Espey, and David A Wink. "A rapid, simple spectrophotometric method for simultaneous detection of nitrate and nitrite". In: *Nitric oxide* 5.1 (2001), pp. 62–71.

[110] Jan-Henrich Rotthauwe, Karl-Paul Witzel, and Werner Liesack. "The ammonia monooxygenase structural gene amoA as a functional marker: molecular fine-scale analysis of natural ammonia-oxidizing populations". In: *Applied and environmental microbiology* 63.12 (1997), pp. 4704–4712.

[111] Ricardo J Eloy Alves et al. "Nitrification rates in Arctic soils are associated with functionally distinct populations of ammonia-oxidizing archaea". In: *The ISME journal* 7.8 (2013), pp. 1620–1631.

[112] Alma E Parada, David M Needham, and Jed A Fuhrman. "Every base matters: assessing small subunit rRNA primers for marine microbiomes with mock communities, time series and global field samples". In: *Environmental microbiology* 18.5 (2015), pp. 1403–1414.

[113] Amy Apprill et al. "Minor revision to V4 region SSU rRNA 806R gene primer greatly increases detection of SAR11 bacterioplankton". In: *Aquatic Microbial Ecology* 75.2 (2015), pp. 129–137.

[114] Petra Pjevac et al. "An economical and flexible dual barcoding, two-step PCR approach for highly multiplexed amplicon sequencing". In: *Frontiers in microbiology* 12 (2021), p. 669776.

[115] Benjamin J Callahan et al. "DADA2: High-resolution sample inference from Illumina amplicon data". In: *Nature methods* 13.7 (2016), pp. 581–583.

[116] Christian Quast et al. "The SILVA ribosomal RNA gene database project: improved data processing and web-based tools". In: *Nucleic acids research* 41.D1 (2012), pp. D590–D596.

[117] Holger Daims et al. "In situ characterization of Nitrospira-like nitrite-oxidizing bacteria active in wastewater treatment plants". In: *Applied and environmental microbiology* 67.11 (2001), pp. 5273–5284.

[118] Dumsane Themba Matse et al. *Copper induces nitrification by ammonia-oxidizing bacteria and archaea in pastoral soils*. Tech. rep. Wiley Online Library, 2023.

[119] Huan He et al. “Influence of Cu application on ammonia oxidizers in fluvo-aquic soil”. In: *Geoderma* 321 (2018), pp. 141–150.

[120] Bruna G Oliveira et al. “Soil pH does not interfere with nitrification inhibitor efficiency for reducing N2O emissions from soils treated with concentrated vinasse and urea”. In: *Geoderma* 426 (2022), p. 116087.

[121] Maria Tourna et al. “Growth, activity and temperature responses of ammonia-oxidizing archaea and bacteria in soil microcosms”. In: *Environmental Microbiology* 10.5 (2008), pp. 1357–1364.

[122] Hussnain Mukhtar et al. “Relative abundance of ammonia oxidizing archaea and bacteria influences soil nitrification responses to temperature”. In: *Microorganisms* 7.11 (2019), p. 526.

[123] Kristina Schauss et al. “Dynamics and functional relevance of ammonia-oxidizing archaea in two agricultural soils”. In: *Environmental Microbiology* 11.2 (2009), pp. 446–456.

[124] Ruo-Nan Wu et al. “A more comprehensive community of ammonia-oxidizing archaea (AOA) revealed by genomic DNA and RNA analyses of amoA gene in subtropical acidic forest soils”. In: *Microbial ecology* 74 (2017), pp. 910–922.

[125] Ju-pei Shen et al. “Abundance and composition of ammonia-oxidizing bacteria and ammonia-oxidizing archaea communities of an alkaline sandy loam”. In: *Environmental microbiology* 10.6 (2008), pp. 1601–1611.

[126] Sara Hallin et al. “Relationship between N-cycling communities and ecosystem functioning in a 50-year-old fertilization experiment”. In: *The ISME journal* 3.5 (2009), pp. 597–605.

[127] Ella Wessén and Sara Hallin. “Abundance of archaeal and bacterial ammonia oxidizers–possible bioindicator for soil monitoring”. In: *Ecological Indicators* 11.6 (2011), pp. 1696–1698.

[128] Zhibin Wang et al. “Dosage-Dependent Toxicity of Universal Solvent Dimethyl Sulfoxide to the Partial Nitrification Wastewater Treatment Process”. In: *ACS ES&T Water* 3.3 (2023), pp. 848–856.

[129] JM Bremner and LG Bundy. “Inhibition of nitrification in soils by volatile sulfur compounds”. In: *Soil Biology and Biochemistry* 6.3 (1974), pp. 161–165.

[130] Anne Saari and Pertti J Martikainen. “Differential inhibition of methane oxidation and nitrification in forest soils by dimethyl sulfoxide (DMSO)”. In: *Soil Biology and Biochemistry* 33.11 (2001), pp. 1567–1570.

[131] Paulo Cesar Ocheuze Trivelin et al. “Nitrogen losses of applied urea in the soil-plant system during two sugar cane cycles”. In: *Pesquisa Agropecuária Brasileira* 37 (2002), pp. 193–201.

[132] Paul J Crutzen et al. “N 2 O release from agro-biofuel production negates global warming reduction by replacing fossil fuels”. In: *Paul J. Crutzen: A pioneer on atmospheric chemistry and climate change in the anthropocene* (2016), pp. 227–238.

[133] Jan Willem Erisman et al. “The Dutch N-cascade in the European perspective”. In: *Science in China Series C: Life Sciences* 48 (2005), pp. 827–842.

[134] Will Steffen et al. “Planetary boundaries: Guiding human development on a changing planet”. In: *science* 347.6223 (2015), p. 1259855.

[135] Johan Rockström et al. “Planetary boundaries: exploring the safe operating space for humanity”. In: *Ecology and society* 14.2 (2009).

[136] Katherine Richardson et al. “Earth beyond six of nine planetary boundaries”. In: *Science advances* 9.37 (2023), eadh2458.